Combined Chemical Looping Combustion and Calcium Looping for Enhanced Hydrogen Production from Biomass Gasification

By

Ryad Abdul Rahman

Thesis submitted to the Faculty of Graduate and Postdoctoral Studies

In partial fulfillment of the requirements for the degree of

M.A.Sc. in Chemical Engineering

Department of Chemical and Biological Engineering

University of Ottawa

October 2014

Acknowledgments

I would first like to express my gratitude to my co-supervisors Dr. Poupak Mehrani, Dr. Edward J. Anthony and Dr. Arturo Macchi for their guidance and support during the course of my studies. Their encouragements and the high standards they exhibited and constantly demanded from me were paramount to making the last two years a fruitful learning experience.

I am grateful to Robert Symonds and Dr. Dennis Lu from CanmetENERGY for providing me with their expertise and support. The insight they provided was invaluable. I would also like to thank Dr. Firas Ridha for mentoring me on operating much of the equipment used during the course of my research.

Special thanks go to the Ontario Ministry of Training, Colleges and Universities as well as to Natural Sciences and Engineering Research Council of Canada for the funding support they provided.

Lastly, I want to thank my family and friends for their unflinching support and encouragement throughout my studies.

Abstract

Production of hydrogen from biomass steam gasification can be enhanced by using calcium oxide sorbents for CO_2 capture in the gasifier. Calcium looping suffers from two main drawbacks: the need for high-purity oxygen in order to regenerate the sorbent under oxy-fuel combustion conditions and the loss of sorbent reactivity over several cycles due to sintering of pores upon calcination at high temperatures. One method of addressing the issue of oxygen supply for calcination in calcium looping is to combine the calcium looping and chemical looping processes, where the heat produced by the reduction of an oxygen-carrier by a fuel such as natural gas or gasification syngas, drives the calcination reaction. The technologies can be integrated by combining an oxygen carrier such as CuO with limestone within a composite pellet, or by cycling CuO and limestone within distinct particles. The goal of this project is thus to investigate the different sequences of solids circulation and the cyclic performance of composite limestone-CuO sorbents under varied operating conditions for this novel process configuration.

Using a thermogravimetric analyzer (TGA), it was found that using composite CaO/CuO/alumina-containing cement pellets for gasification purposes required oxidation of Cu to be preceded by carbonation (Sequence 2) as opposed to the post-combustion case where the pellets are oxidized prior to carbonation (Sequence 1). Composite pellets were tested using Sequence 2 using varying carbonation conditions over multiple cycles. While the pellets exhibited relatively high carbonation conversion, the oxidation conversion underwent a decrease for all tested conditions, with the reduction in oxygen uptake particularly drastic when the pellets were pre-carbonated in the presence of steam. It appears that the production of a layer of $CaCO_3$ fills up the pellets pores, obstructing the passage of O_2 molecules to the more remote Cu sites. Limestone-based pellets and Cu-based pellets were subsequently tested in separate CaL and CLC loops respectively to assess their performance in a dual-loop process (Sequence 3). A maximum Cu content of 50% could be accommodated in a pellet with calcium aluminate cement as support with no loss in oxidation conversion and no observable agglomeration.

Sommaire

Il est possible de hausser le rendement d'hydrogène dans un gazéifieur en captant le CO_2 à travers l'utilisation de sorbants à base de CaO. La technologie basée sur les réactions cycliques de carbonation et calcination requiert de l'oxygène pur pour régénérer le sorbant à travers la combustion oxy-combustible, et les sorbants utilisés deviennent moins réactifs à chaque cycle en raison de la fusion des pores à hautes températures. Cette technologie peut être combinée avec celle de combustion en boucle chimique de façon à ce que la chaleur dégagée par la réduction d'un oxyde métallique par l'entremise de gaz naturel ou d'un gaz de synthèse soit utilisée pour la calcination. Une telle intégration peut être accomplie en granulant un oxyde métallique tel le CuO avec du calcaire, ou en opérant avec ces deux matériaux séparés en deux particules distinctes. L'objectif de cette étude est donc d'évaluer les différentes configurations possibles ainsi que d'évaluer la performance de granulés composés de CuO et de calcaire à différentes conditions d'opération lors de nombreux cycles.

En utilisant un TGA, il fut possible d'établir que l'utilisation de granulés composés de CuO, CaO et ciment à base d'alumine pour la gazéification requérait que l'oxydation du Cu soit précédée par la carbonation (Séquence 2), contrairement au cas de postcombustion qui nécessite l'ordre inverse (Séquence 1). La performance des granulés à travers la Séquence 2 fut étudiée sur de nombreux cycles à différentes conditions de carbonation. Bien que la conversion cyclique de CaO demeura relativement haute, la conversion de Cu lors de l'oxydation subit une baisse à toutes les conditions testées, particulièrement lorsque la carbonation eut eu lieu en présence de la vapeur d'eau. Il semblerait que la formation d'une couche volumineuse de $CaCO_3$ bloque les pores dans les granulés, obstruant ainsi le passage des molécules d'O_2 en direction des particules de Cu. Des granulés exclusivement à base de CaO et de Cu furent testés dans les boucles individuelles de CaL et CLC respectivement afin d'évaluer leurs performances dans un procédé à boucle double (Séquence 3). La teneur maximum en cuivre dans les granulés sans qu'il soit possible d'observer de l'agglomération ou de perte de conversion d'oxydation est de 50%.

Table of Contents

List of Tables

List of Figures

Nomenclature

$m_{carb}(0)$	mass of the sorbent prior to the carbonation stage
$m_{carb}(t)$	mass of the sorbent at a time *t* after start of carbonation
$m_{oxi}(0)$	mass of the pellet before the start of oxidation
$m_{oxi}(t)$	mass of the sorbent at a time *t* from the onset of oxidation
m^0_{sample}	mass of the calcined sorbent preceding the carbonation and oxidation stages
MM_{CaCO_3}	molar mass of $CaCO_3$
MM_{CaO}	molar mass of CaO
MM_{Cu}	molar mass of Cu
MM_{CuO}	molar mass of CuO
x_{CaO}	mass fraction of CaO in the sorbent
x_{Cu}	mass faction of Cu in the sorbent
X_{Carb}	carbonation conversion
X_{Oxi}	oxidation conversion
ΔH^r_T	enthalpy of reaction at temperature *T*

Acronyms

BET	Brunauer-Emmett-Teller
BJH	Barrett-Joyner-Halenda
CaL	Calcium Looping
CLC	Chemical Looping Combustion
TGA	Thermogravimetric Analyzer
XRD	X-Ray Diffraction
XRF	X-Ray Fluorescence

Chapter 1 Introduction

Fossil fuels are still heavily relied upon to meet the ever-increasing energy demands. According to the latest report from the International Energy Agency (IEA), more than 80 % of the world energy supply is fossil-based (IEA, 2013). With the existing infrastructures to process coal firmly entrenched and the current low price of fuels such as natural gas, it is expected that fossil fuel allocation within the global energy supply will remain largely unchanged for the foreseeable future. While maintaining the status quo on fossil fuel use might appear economically sound, the resulting long-term environmental outlook is far more questionable, given that thermal conversion of fossil fuels generates significant amounts of greenhouse gas (GHG) emissions. Greenhouse gases absorb infrared radiation from the sun, effectively preventing it from being reflected to outer space and confining heat to the earth's atmosphere. While greenhouse gases comprise CH_4, CO_2, N_2O and water vapour, CO_2 accounts for more than 90% of all GHG emissions, and its concentration in the atmosphere has increased from 278 ppm in 1750 to 390.5 ppm in 2011 (IPCC, 2013). It is noteworthy that the average air temperature has increased by about 0.6°C since 1860 (Salinger, 2005). While the causality between these two phenomena is still debated, it is undeniable that significantly increased CO_2 levels in the Earth's atmosphere have been recorded since the advent of the industrial revolution (Canadell et al., 2007), a period which triggered wide-scale use of fossil fuels.

Bending the current trend can be accomplished through two main strategies. Decarbonizing the energy sector will require an increasing share of renewable sources of energy such as solar, wind, hydroelectric, biomass and nuclear at the expense of fossil fuels. The other channel for change is through carbon capture and storage (CCS). CCS involves capturing CO_2 produced as a

result of fossil fuel combustion or gasification, pressurizing it to more than 100 atm and storing it within geological sites from which it cannot escape back to the atmosphere (Boot-Handford et al., 2013).

It is believed in some circles that decarbonization of the energy supply might be accomplished through the implementation of a "hydrogen energy economy", a system involving the production of hydrogen through renewable sources and its use to cater to the energy demand, particularly in the domain of transportation. Although hydrogen is already used as a fuel in the aerospace industry to power rocket engines, its utilization for everyday transportation is still being researched intensively. In addition, presently one of hydrogen primary industrial uses is in the petroleum industry for oil refining (Ramachandran & Menon, 1998). Given that the amount of refined oil produced through the oil sands is set to triple by 2020 (Isaacs, 2008), a corresponding increasing demand for hydrogen will in all likelihood be required. Paradoxically, while hydrogen itself is marketed as a clean fuel, more than 95 % of hydrogen production is carried out through the use of fossil fuels, primarily through steam methane reforming (Ewan & Allen, 2005). A clean, carbon-neutral alternative to hydrogen production from fossil fuels comes in the form of biomass gasification. Not only is biomass a renewable resource, but it is also vastly abundant in Canada; an equivalent of 5.1×10^9 GJ worth of wood residues and pellets is harvested every year in Canada, with more than 80 % of the 1,000,000 tonnes of wood pellets produced exported to Europe (Magelli et al., 2009). The implementation of biomass gasification at an industrial scale could shift a significant share of those exported wood pellets towards local use for gasification purposes, If biomass gasification is coupled with a carbon capture and storage technology,

biomass gasification can even be considered carbon-negative, and effectively help decreasing the amount of CO_2 in the atmosphere.

Of the numerous technologies that have been proposed to capture CO_2 as part of a CCS process, amine scrubbing is probably the one closest to being integrated with combustion/gasification processes on an industrial scale, given that it is already applied commercially to strip CO_2 from natural gas in numerous plants (Rochelle, 2009). However, the technology faces some issues; it is subject to significant energy penalties, making it a costly process (Romeo et al., 2008), and the amine decomposes at high temperatures and is irremediably deactivated by reaction with gases such as oxygen and sulfur dioxide (Olajire, 2010). Should it be integrated with biomass gasification, amine scrubbing could only be implemented as an "end of pipe" application, where it would absorb the CO_2 from a produced gas stream. The technology involves the reaction of the amine-based solvent with CO_2 close to ambient temperature, while its regeneration takes place at 100-120°C (Rochelle, 2009), conditions far from those suitable for biomass gasification, making in-situ CO_2 capture using this particular method impossible. Given that biomass gasification is carried out at high temperatures (typically above 600°C and often much hotter), the produced gas would require significant cooling before any CO_2 absorption could be attempted.

Another carbon capture technology which is touted as being more energy efficient and less expensive is calcium looping (Abanades et al., 2004), which involves the reaction of CaO with CO_2 at moderately high temperatures (>600°C). Limestone, a natural and abundant sedimentary rock, is a relatively cheap source of CaO. In addition to the efficiency and economic advantages that it holds over amine scrubbing, calcium looping enables the capture of CO_2 at conditions that

overlap with those at which biomass gasification takes place (600-750°C at atmospheric pressure) making the combination of both technologies in an in-situ carbon capture process implementable. The benefits of such integration will be discussed in detail in Section 1.2.

1.1 Biomass Gasification

Biomass is organic matter formed through the conversion of solar energy to chemical energy through photosynthesis, and encompasses both energy crops and waste materials. Different types of biomass can have vastly different compositions, but they generally all consist of elevated moisture content, a fibrous structure composed of lignin, carbohydrates or sugars and ash (Turn, 1999). Woody energy crops, herbaceous energy crops, mill wood waste and animal waste are a few examples of biomass that illustrate the diversity of this resource (Florin & Harris, 2008).

Biomass gasification is the thermochemical conversion of biomass at elevated temperatures (500°C-1400°C) using a gasifying agent such as air, oxygen, steam or carbon dioxide to produce a mixture of gases composed mainly of carbon monoxide and hydrogen, together with smaller quantities of carbon dioxide, methane, steam, higher hydrocarbons and nitrogen (Ciferno and Marano, 2002). Although direct combustion of biomass is technically easier, gasification is advantageous in that it can exploit low-value feedstock not only to produce electricity, but also fuels that can be utilized subsequently for transportation purposes (Kumar et al., 2009). The wide distribution of gaseous species evolved during steam gasification is a result of both gas-solid reactions between the steam and biomass and gas-gas reactions between the formed gases and the fed steam. The decomposition of biomass through gasification occurs through three stages, in order of increasing temperature: (i) pyrolysis (300-500°C) (ii) cracking and reforming (>600°C) (iii) char gasification (>800°C) (Florin & Harris, 2008). Of the three listed stages, the cracking

and reforming reactions are the most important at determining the final composition of the gas produced (Antal et al., 1984). The main reactions involved during the steam gasification of biomass are shown in Table 1.1.

Table 1.1 Main reactions occurring during biomass gasification.

Name of Reaction	Chemical reaction	$\Delta H^{r}_{923\,K}$ (kJ/mol)	Reaction Number
Biomass reforming	$C_nH_mO_p + (2n-p)H_2O \rightarrow nCO_2 + (\frac{m}{2} + 2n - p)H_2$	-	(1.1)
Water-gas shift	$CO + H_2O \leftrightarrow CO_2 + H_2$	-35.6	(1.2)
Methane reforming	$CH_4 + H_2O \leftrightarrow CO + 3H_2$	+224.8	(1.3)
Water-gas (i)	$C + H_2O \leftrightarrow CO + H_2$	+135.8	(1.4)
Water-gas (ii)	$C + 2H_2O \leftrightarrow CO_2 + 2H_2$	-100.3	(1.5)
Oxidation (i)	$C + O_2 \leftrightarrow CO_2$	-394.5	(1.6)
Oxidation (ii)	$C + 0.5O_2 \leftrightarrow CO$	-111.5	(1.7)
Reverse Boudouard	$C + CO_2 \leftrightarrow 2CO$	+171.4	(1.8)
Methanation	$C + 2H_2 \leftrightarrow CH_4$	-88.9	(1.9)

The final produced gas distribution depends on a number of parameters. Ciferno & Marano (2002) compiled data from a number of sources in their study and reported a wide spectrum of gaseous product distributions, with the minimum and maximum hydrogen contents of 4.1% and 43.3 %, respectively. The process detailed various reactor designs, gasifying agents, types of biomass, temperatures, steam-to-biomass ratios and pressures, parameters which are paramount in determining the final composition of the produced gas.

For example, while air, oxygen, steam or their mixtures can all be used as gasifying agents, it has been shown that the use of steam results in a higher yield of hydrogen in the produced syngas

(Udomsirichakorn & Salam, 2014). Not only is the H_2O fed broken down into supplementary H_2, but as opposed to air-based gasification, the resulting gas mixture is devoid of nitrogen and therefore holds a higher heating value (Franco et al., 2003). Herguido et al. (1992) further noted in their study that a higher steam-to-biomass ratio was correlated with a reduction in tar and char yield, meaning that in addition to being an essential parameter in terms of gaseous distribution, it can also provide other operational benefits.

Biomass gasifiers can be classified in four main categories: updraft fixed bed, downdraft fixed bed, bubbling fluidized bed and circulating fluidized beds. Due to their propensity to produce significant amounts of tar and unconverted char respectively, updraft and downdraft fixed bed gasifiers are seldom used; instead the majority of biomass gasifiers currently being developed make use of either bubbling fluidized bed or a circulating fluidized bed technology (Ciferno & Marano, 2002). Another primary advantage fluidized bed gasifiers hold over their fixed bed counterparts is that the temperature within the former is distributed uniformly along the gasification zone (Couto et al., 2013).

While all the aforementioned factors will affect the final hydrogen content of the produced gas to various extents, most literature sources list the maximum hydrogen yield as falling between 40 and 50% (Franco et al. 2003; Herguido et al., 1992; Turn et al. 1998; Walawender et al., 1985) , which is probably too low for commercial applications. Those low yields also make the process uneconomic, given that just the cost of the biomass feedstock can amount to up to 40% of the cost of H_2, and separating H_2 in a synthetic gas from impurities such as CO and CH_4 incurs significant expenses. In order to increase the yield of H_2 in the produced gas, a CO_2 sorbent can

be employed in-situ to capture CO_2 during gasification resulting in the thermodynamic equilibrium of the water-gas shift reaction to move towards the products side, enhancing H_2 production.

1.2 Calcium Looping

On the basis of technical viability and economic feasibility, it can be argued that the best suited technique for in-situ CO_2 capture in a biomass gasifier is calcium looping using CaO-based sorbents (Florin & Harris, 2008). The CaL cycle is based on the following reversible reaction:

$$CaO_{(s)} + CO_{2(g)} \leftrightarrow CaCO_{3(s)} \qquad \Delta H^{r}_{650^{\circ}C} = -171\, kJ/mol \tag{1.10}$$

Not only can CaO react with CO_2 within a temperature window shared with biomass gasification, but since it can be derived from a variety of natural precursors such as limestone and dolomite, it is an abundant and cheap material. Moreover, calcium looping employs fluidized bed technology which, as established in Section 1.2, is the leading technology among gasifiers being currently developed. Although fluidized beds will usually be composed of inert material such as alumina or sand, limestone has also been used in biomass gasifiers. The bubbling fluidized bed gasifier developed by Manufacturing and Technology Conversion International (MTCI) was reported to generate a product with considerably higher hydrogen content using a limestone bed (45.86%) as opposed to a sand bed (35.06 %) (Ciferno & Marano, 2002).

The integration of calcium looping with steam biomass gasification, illustrated in Figure 1.1, holds numerous incentives in addition to enhancement of H_2 content in the produced gas. Since the carbonation of CaO in the gasifier would be exothermic, the heat released can be used to partially drive the endothermic gasification process. Part of the required heat can also be supplied by the sensible heat of the solids exiting the calciner, which is operated at high temperature (>900°C). The water-gas shift reaction is mildly exothermic, and its enhancement will also contribute some of the heat required by the endothermic gasification process. Moreover, CaO has been shown to display catalytic behaviour in the decomposition of tar at high temperatures (Florin & Harris, 2008).

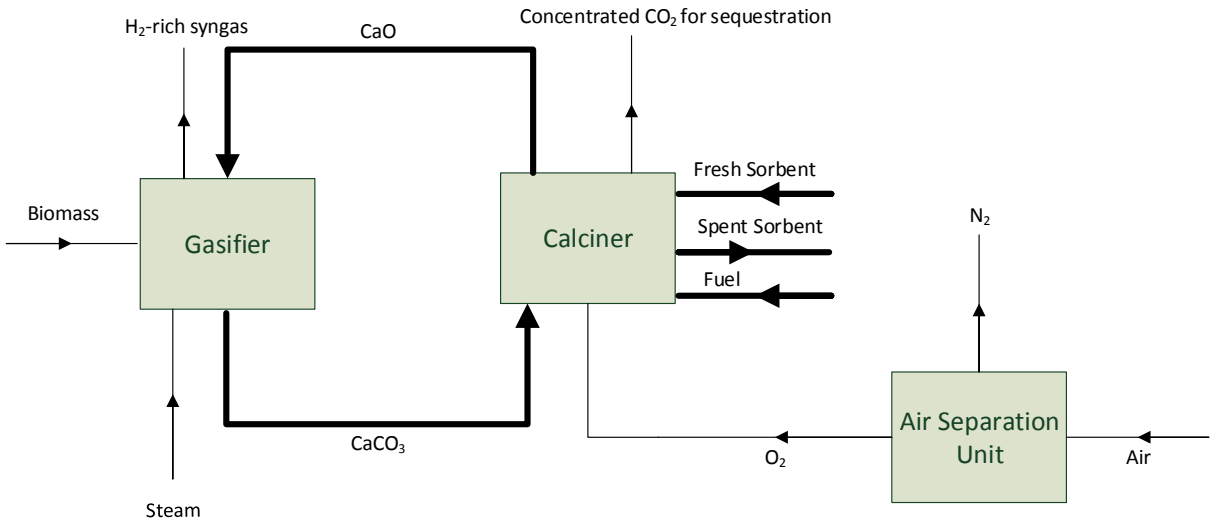

Figure 1.1 Schematic of combined steam biomass gasification with calcium looping

The exothermic nature of the carbonation of CaO causes it to be thermodynamically more favorable at lower temperatures, but it is usually carried out at >600°C in order for the reaction to proceed at a reasonable rate. Carbonation of CaO proceeds first through a fast reaction-controlled stage, followed by a slower diffusion-limited step. A typical carbonation-calcination

cycle, where CaO starts to react with CO_2 at the 15 minute mark, is shown in Figure 1.2. The reaction-controlled stage is characterized by the unobstructed access of CO_2 molecules to the surface of active CaO sites, whose carbonation leads to the formation of a $CaCO_3$ layer. $CaCO_3$, with a molar volume of 36.9 cm^3/g, occupies significantly more volume than porous CaO (16.9 cm^3/g), which implies that for every gram of CaO carbonated, 20 cm^3 of newly formed material need to be accommodated within the sorbent structure. Therefore, as the active surface sites are carbonated, the passage of CO_2 through the sorbent becomes increasingly restricted as further carbonation requires CO_2 molecules to diffuse through the newly formed voluminous $CaCO_3$ shell covering the more remote unreacted CaO sites. This second, diffusion-limited stage is therefore considerably slower than the first stage and if allowed the required time, theoretically proceeds until complete conversion is achieved. Contrastingly, the calcination of $CaCO_3$ is governed by fast kinetics at the required high temperatures (>900°C).

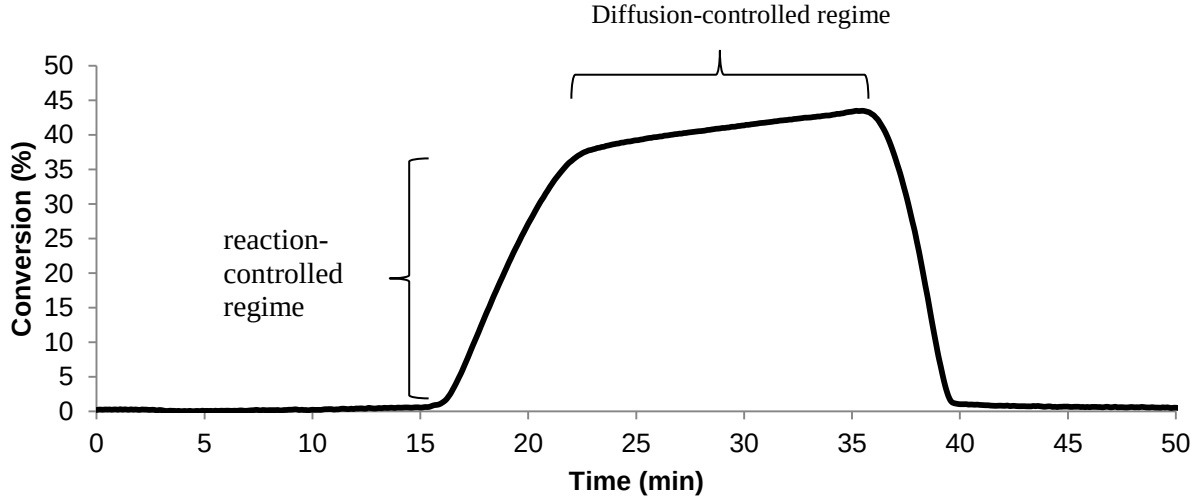

Figure 1.2 Example of a typical carbonation-calcination cycle with CaO pellets in 8% CO_2 and balance N_2 after calcination at 850°C in N_2

The equilibrium vapour pressure of CO_2 over CaO can be determined at various temperatures using the relationship proposed by Baker (1962), shown by equation (1.11). The corresponding plot of equilibrium vapour pressure of CO_2 vs. temperature is given in Figure 1.3.

$$\log P_e\ (atm) = 7.079 - \frac{38{,}000}{4.574\ T(K)} \tag{1.11}$$

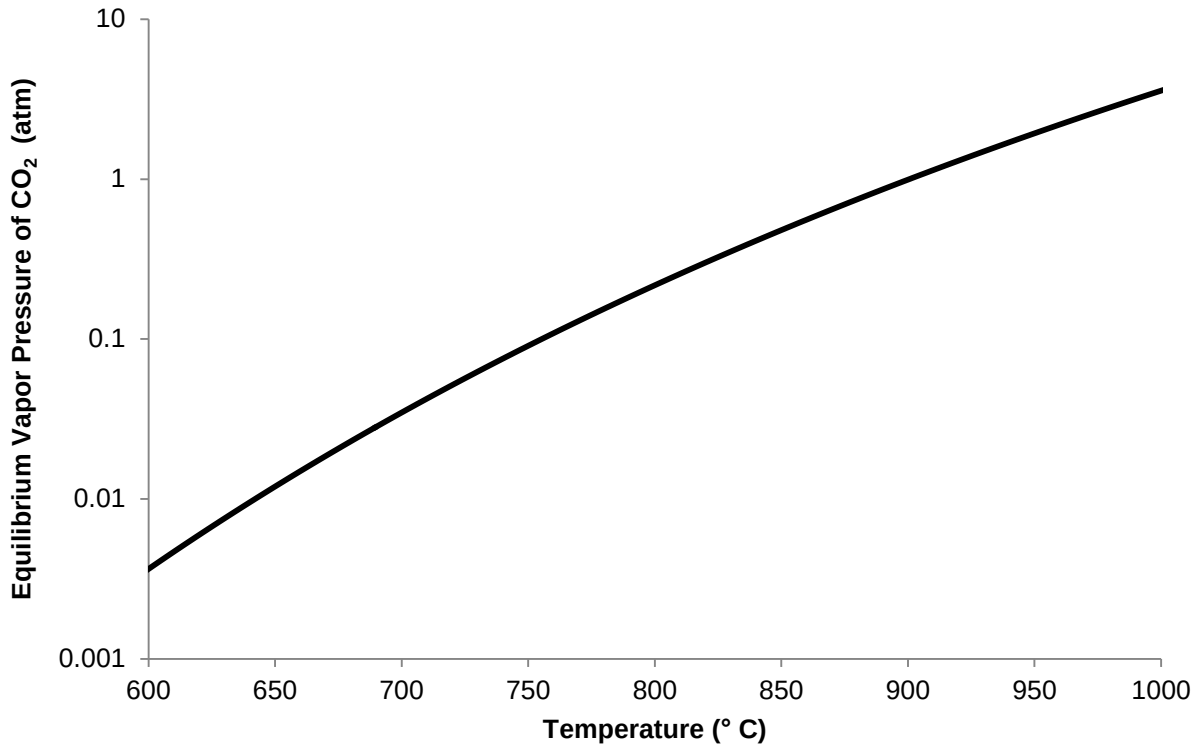

Figure 1.3 Equilibrium vapor pressure of CO_2 over CaO as a function of temperature through chemical sorption of CO_2 on CaO (Baker, 1962)

In a calcium looping process, the lime-based sorbent circulates between two vessels: the carbonator, where CaO reacts with CO_2 to form $CaCO_3$, and the calciner, where the reverse reaction takes place to regenerate CaO (Blamey et al., 2010). From the relationship provided by Baker, it can be shown that carbonation of CaO at 650°C results in a CO_2 vapour pressure of 0.012 atm. This means that if a hypothetical flue gas containing CO_2 was passed through a bed of

calcined limestone at atmospheric pressure, the carbonation reaction at those conditions would lead the resulting gas to exit the system with a minimum CO_2 content of 1.2 %.

In order to generate a highly concentrated stream of CO_2 suitable for compression and sequestration during the calcination step, the latter needs to be carried out at a high temperature; according to Baker (1962), for a CO_2 vapour pressure of 1 atm, the equilibrium temperature is 900°C. The heat required to operate the calciner at such conditions and to raise the temperature of incoming solids from the carbonator is generated from the combustion of a suitable fuel, such as biomass or natural gas/coal, in the calciner. If the CO_2 produced from calcination of $CaCO_3$ is to be captured and stored, it is essential that it exits the calciner as a highly concentrated CO_2 stream, or along with an easily separable species such as steam. This requirement precludes the use of air for fuel combustion and instead entails the use of high-purity oxygen for this purpose. The calciner therefore needs to be operated as an oxygen-fired (oxyfuel) combustor. Oxyfuel combustion requires considerable amounts of oxygen with purities typically higher than 95 % (Buhre et al. 2005), produced through cryogenic distillation by an air separation unit. As the high-purity oxygen is used for combustion of the fuel, part of the resulting CO_2-rich flue gas is recycled to the calciner to provide flame moderation and serve as fluidizing agent.

Calcium looping faces a few challenges. Although oxyfuel combustion makes the regeneration of CaO possible while producing a CO_2-rich stream, its reliance on a costly and energy-intensive air separation unit imposes a significant energy penalty on the process (Abanades et al., 2007). The need to circulate significant amounts of solids between different thermal and chemical environments makes the use of a dual fluidized bed combustion (FBC) reactor ideal for this

process (Manovic & Anthony, 2010a). While circulating fluidized beds, by reason of their excellent bed mixing, result in amplified heat and mass transfer and reaction rates, attrition of the particles has been shown to be a major issue in such reactors, resulting in sorbent elutriation (Lu et al., 2008). More critically, exposing the limestone-based sorbent to the high temperatures required in the calciner makes it liable to sintering, a phenomenon through which smaller pores fuse together to form larger pores. The amalgamation of smaller pores results in a decrease in porosity, which diminishes the surface area available for carbonation of CaO to take place and effectively causes the loss in reactivity of the sorbent (Blamey et al. 2010). Sintering is one of the main causes of sorbent deactivation along with fuel ash deposition on the sorbent surface (Hughes et al., 2009) and reaction with syngas or flue gas impurities such as SO_2 (Manovic et al., 2008). In order to keep capturing the same amount of CO_2 from one cycle to the next, spent sorbent needs to be replaced by fresh limestone in the calciner. The rate at which fresh sorbent needs to be added to the system depends on the rate of deactivation of the sorbent in the system; the faster the decay in performance, the higher the fresh sorbent make-up rate will be, and by association, the higher the operational costs of the system.

A plethora of methods have been attempted to counter the loss in CaO reactivity throughout the years, including acid treatment, pelletization with calcium aluminate cement and steam-enhanced carbonation. In particular, the use of calcium aluminate cement as a binder to produce limestone-based pellets has not only been proved to be effective in maintaining high residual activity, but also has resulted in stronger particles, better capable of resisting attrition and subsequent elutriation (Manovic & Anthony, 2010a). Although most techniques were successful to various

degrees in slowing down the decrease in carbonation conversion, the decline in CO_2 uptake has proved to be inexorable, irrespective of any applied method.

Ultimately, the extent of the loss in CaO reactivity depends primarily on the conditions under which calcination is carried out, as well as its duration. In addition to temperature, the nature of the gases involved during calcination also affects the sorbent reactivity in the subsequent cycle. The key therefore to a more durable calcium looping sorbent could come as a combination of different approaches which would include both sorbent modification techniques and ways of making the regeneration process milder, either through a lower calcination temperatures and/or through an increase in the steam content at the expense of CO_2.

1.3 Chemical Looping Combustion

Chemical looping combustion is a relatively new technology which involves circulating a metal oxide, or oxygen carrier, between two vessels: a fuel reactor, where the metal oxide releases its oxygen to burn the fuel fed, and an air reactor, where the metal is oxidized by air to form the metal oxide again. A schematic of a simplified CLC process is provided in Figure 1.4.

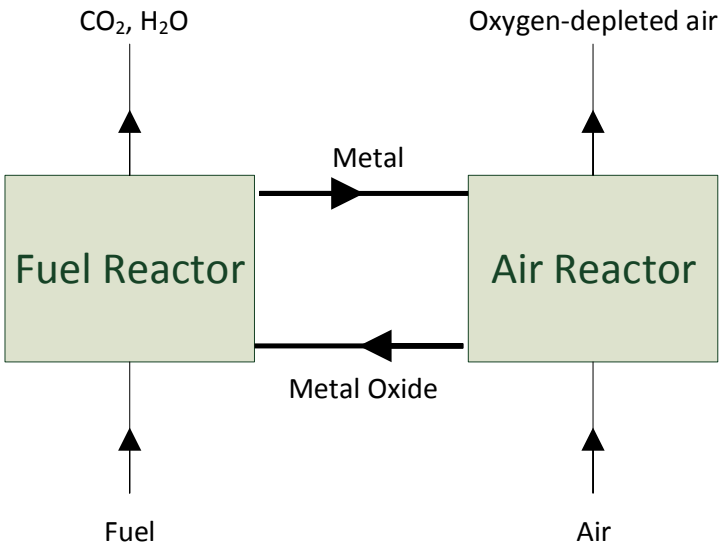

Figure 1.4 Typical CLC process

One major feature of CLC that makes it such an enticing process is the inherent ability to separate oxygen from air without the need for cryogenic distillation. The necessity for an air-separation unit is one of the major drawbacks of oxyfuel combustion, and CLC ability to transport oxygen to the fuel while bypassing such a requirement makes it a promising alternative. While gaseous hydrocarbons or hydrogen are fuels that can easily be used in a CLC process, integration of solid fuels such as coal poses a challenge due to the inherently slow nature of solid-solid reactions as well as formation of ash which inevitably comes into contact with the oxygen-carrier (Imtiaz et al., 2013).

The idea of utilizing the heat produced through a CLC process for an endothermic reaction such as calcination without the need for combustion with fire was first put forward by Lyon & Cole (2000). Incorporating a CLC oxygen carrier with lime is advantageous in the sense that the heat produced by the reduction of an oxygen carrier by a fuel such as natural gas or syngas drives the calcination reaction, avoiding the need for an expensive air separation unit to provide high-purity

oxygen (Manovic & Anthony, 2011b). In such a scenario, however, it is essential for the reduction of the oxygen carrier to be exothermic, which imposes a restriction on the oxygen carriers that can be used in such an integrated process. While several metal oxides can potentially act as oxygen carriers, two of the most promising oxygen-carriers exhibiting exothermic reduction include CuO and MnO_2 (Manovic & Anthony, 2011a). Manovic and Anthony (2011a) incorporated both materials in Al_2O_3-supported composite pellets with CaO as part of the first experimental demonstration of the integration of CLC with CaL. They showed that CuO displayed more promise than MnO_2 as an oxygen-carrier, and reacted exothermically with CO, H_2 and CH_4 as shown by reactions (1.12), (1.13) and (1.14).

$$CuO_{(s)} + \frac{1}{4}CH_{4(g)} \leftrightarrow Cu_{(s)} + \frac{1}{4}CO_{2(g)} + \frac{1}{2}H_2O_{(g)} \qquad \Delta H^r_{900°C} = -52.2\ kJ/mol \qquad (1.12)$$

$$CuO_{(s)} + H_{2(g)} \leftrightarrow Cu_{(s)} + H_2O_{(g)} \qquad \Delta H^r_{900°C} = -100.3\ kJ/mol \qquad (1.13)$$

$$CuO_{(s)} + CO_{(g)} \leftrightarrow Cu_{(s)} + CO_{2(g)} \qquad \Delta H^r_{900°C} = -133.5\ kJ/mol \qquad (1.14)$$

Unlike reduction, which can be either endothermic or exothermic, the oxidation of oxygen carrier metals is always exothermic (Hossain & de Lasa, 2008), and copper is similar in this respect, releasing a significant amount of heat upon reaction with oxygen, as illustrated in equation (1.15).

$$Cu_{(s)} + \frac{1}{2}O_{2(g)} \leftrightarrow CuO_{(s)} \qquad \Delta H^r_{650°C} = -150.7\ kJ/mol \qquad (1.15)$$

Besides its exothermic reduction, Cu offers numerous advantages; compared to other CLC materials, it exhibits high oxygen-carrying capacity (0.20 g O_2/g CuO) and highly reactivity (Manovic & Anthony, 2011b). In addition, while it is more expensive than the more abundant, but less reactive oxygen carriers such as Fe_2O_3, its low cost compared to some other oxygen carriers such as NiO and CoO is plausibly what led (de Diego et al. 2007) to deem CuO one of the cheapest materials available for CLC. Its main downside, however, is its relatively low melting point of 1085°C, which makes it vulnerable to agglomeration at high temperatures, and requires it to be combined with a support (de Diego et al., 2004). A porous support increases the surface area available for reaction, and acts as a binder which enhances the attrition resistance and mechanical strength, while simultaneously augmenting the ionic conductivity of solids (Ishida & Jin, 1994). Al_2O_3 is often used as a support for Cu because of its relatively high abundance (Xu et al., 2013), although other options include SiO_2, ZrO_2, and TiO_2 amongst others (de Diego et al., 2004).

Copper can exhibit both +1 and +2 oxidation states in its oxide form. Copper (II) oxide will decompose to copper (I) oxide and release oxygen at high temperatures (>870°C) and low partial pressure of oxygen (Jerndal et al., 2006), as shown in reaction (1.16).

$$2CuO_{(s)} \leftrightarrow Cu_2O_{(s)} + \frac{1}{2}O_{2(g)} \qquad (1.16)$$

1.4 Integrated Process of CaL-CLC

Although the idea of combining CaL and CLC has existed ever since it was proposed by Lyon & Cole in 2000, attempts to experimentally demonstrate the feasibility of such integration are relatively recent. From 2011 onwards, a number of attempts at combining limestone and copper oxide in an integrated CaL-CLC process have been reported, with all of them loosely following a reactor configuration proposed by Manovic & Anthony (2011b) for post-combustion application. This configuration, illustrated in Figure 1.5, involves, notwithstanding the combustor, 3 reactors, namely the carbonator, the air reactor and the calciner, which also acts as the reducer for CuO.

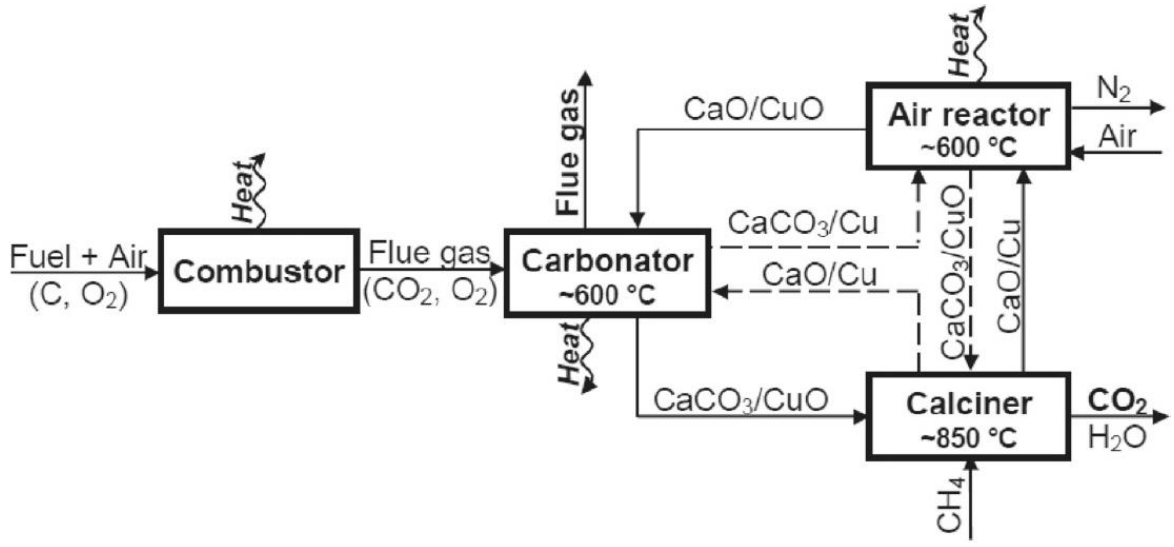

Figure 1.5 Integration of CaL and CLC for post-combustion application, adapted from (Manovic and Anthony 2011b)

Manovic et al. (2011a) synthesized different batches of composite CuO-CaO-Al_2O_3-based-cement pellets using a wet mechanical mixing method. Schematics of the pellets, which were produced both as homogeneous and CuO core-in-CaO-shell pellets, are shown in Figure 1.6.

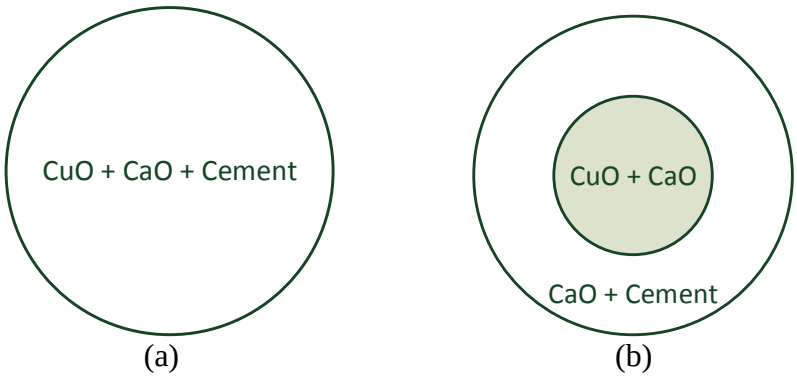

Figure 1.6 Schematic diagram of copper-limestone-calcium aluminate cement pellets. (a) Homogeneous; and (b) Core-in-shell, adapted from (Manovic et al. 2011a)

Both types of pellets were shown to exhibit comparably reasonable performances when exposed to post-combustion process conditions, with high oxidation conversion (10g/ 100g pellets) and high initial CaO conversion (~65%) followed by the typical characteristic decay in CO_2 conversion (Manovic & Anthony, 2011b). However, the pellets were only tested over three carbonation-calcination cycles, leaving it unclear as how they perform over a larger number of cycles.

Using a wet mixing method, Qin et al. (2012) produced a CaO/CuO sorbent supported with MgO with a mass fraction of 11.24 %, 63.76 % and 25 %, respectively, justifying the CaO/CuO molar ratio of 0.25 on the basis of the heat balance between reduction of CuO in methane and calciniation of $CaCO_3$. Although the authors reported that the oxidation conversion was nearly 100 % for 68 cycles tested, they noted that the carbonation conversion of the sorbents containing CuO was significantly lower than that of sorbents consisting solely of CaO and MgO. They attributed the lower performance of composite CuO-CaO-MgO sorbents to the "wrapping" of Cu/CuO around CaO particles.

Kierzkowska & Müller (2012) synthesized three CaO-CuO composite sorbents with CuO/CaO molar ratios of 1:1, 1.3:1 and 3.3:1 using a co-precipitation technique, and subjected them to at least 10 isothermal oxidation/carbonation/calcination-reduction cycles at 750°C. As in other studies, they highlighted the high sustained oxidation conversion (>98 % over all cycles tested). Although the composite sorbent had a lower CO_2 uptake than Havelock limestone on a g of CO_2 per g of sorbent basis, the authors pointed out that the sorbent also experienced a much slower decline in CO_2 uptake than the abovementioned limestone.

1.5 Integration of Combined CaL and CLC with Pre-Combustion Processes

Although the combination of CaL and CLC for post-combustion applications has been shown to be promising, what has not been tried so far is integrating the technology with pre-combustion technologies such as biomass gasification. Given the inherent benefits of in-situ carbon capture for gasification, the carbonator would act as the gasifier in such a process. While just as in the post-combustion scenario, the present system would utilize three distinct reactors (carbonator, air reactor and calciner), questions remain with regards to the best way of circulating solids in such a system. Ideally, the solids would circulate across the different reactors in a similar sequence as in the post-combustion case: carbonator (gasifier)-calciner (fuel reactor)-air reactor, finally return to carbonator (gasifier). This sequence, which for the sake of simplicity will be labelled as Sequence 1, is illustrated in Figure 1.7, where the reactions expected in the process are described below each relevant reactor.

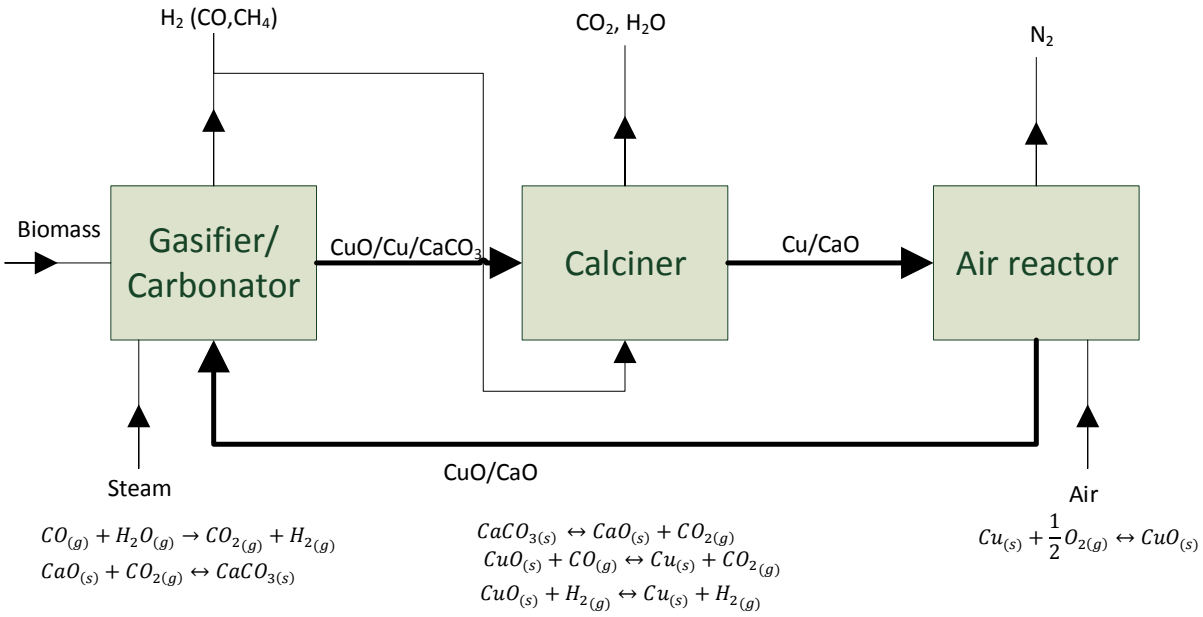

Figure 1.7 Sequence 1: carbonator (gasifier)-calciner-air reactor-carbonator (gasifier) sequence

Contrary to flue gas from fossil fuel combustion which consists primarily of N_2 and CO_2, the producer gas from the steam gasification of biomass is composed, for the most part, of H_2, CO, CO_2 and CH_4, with their relative proportions dependent on the gasifier conditions. Thus, in addition to the carbonation of CaO to $CaCO_3$, significant reduction of CuO to Cu could occur inside the gasifier (carbonator). This depends on the relative kinetics of CaO carbonation and CuO reduction and the residence time of the pellets within the reactor. Manovic & Anthony (2011b) examined this scenario and underlined the fast kinetics of both the reduction of CuO and the carbonation of CaO (specifically the reaction kinetic – controlled regime). However, in their study those reactions were carried out separately (i.e. carbonation in solely CO_2 , followed by parallel reduction/calcination in CO & H_2). Thus, in their case which of the two reactions is faster remains uncertain. While the reduction of CuO could be significant in this particular gaseous environment, there is also the distinct possibility that the fast regime carbonation would

result in the formation of a $CaCO_3$ product layer, impeding the transport of the reducing gases to the CuO core, especially if CuO core-in- CaO shell composite pellets (similar to those employed by Manovic et al. 2011a) are used. If the kinetics of CuO reduction are so fast that it experiences a significant conversion even at limited exposure times to the gasifying mixture, using the sequence illustrated in Figure 1.7 will be challenging. There will subsequently be insufficient CuO to be reduced and generate the required heat to drive the calcination of $CaCO_3$. A different sequence for solids circulation would then be required: carbonator (gasifier)-air reactor-calciner (fuel reactor)-carbonator (gasifier), identified as Sequence 2 and illustrated in

Figure 1.8.

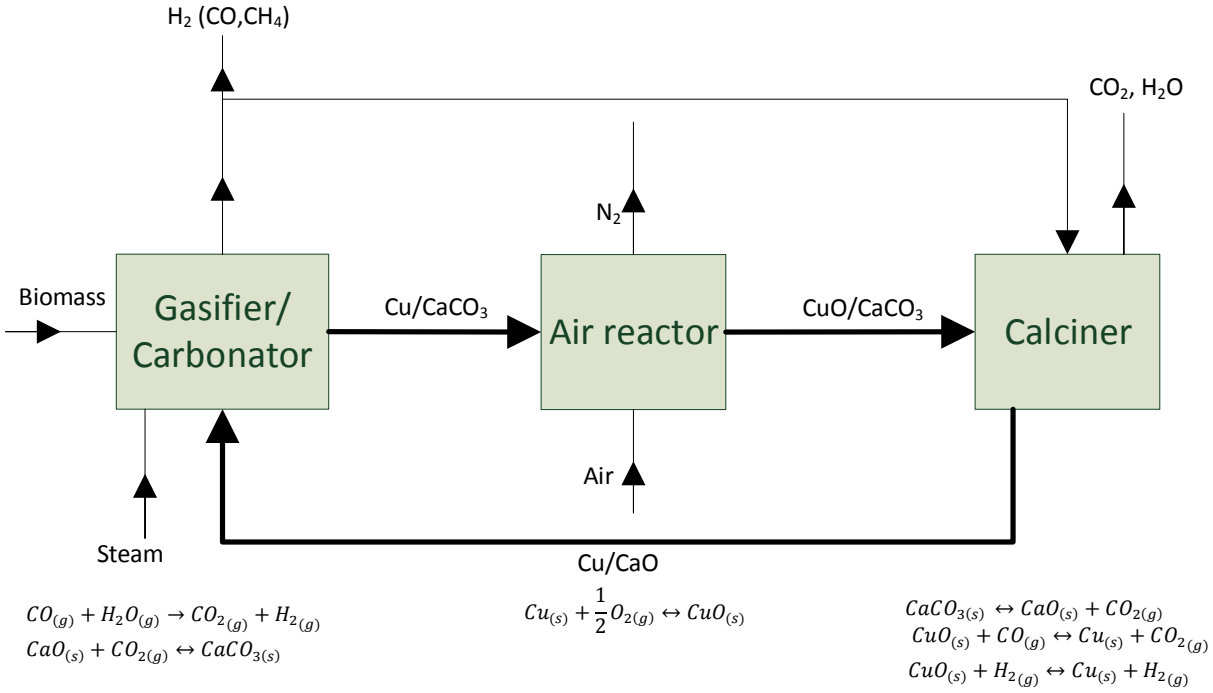

Figure 1.8 Sequence 2: carbonator (gasifier)-air reactor-calciner-carbonator (gasifier) sequence

Given the highly exothermic nature of the oxidation of Cu, ideally the air reactor would be operated at as high a temperature (>950°C) as possible in Sequence 2. The sensible heat of the solids would allow the solids to enter the calciner at a relatively high temperature, which would reduce the fuel requirements in the latter. The main issue with such a scenario is the possible calcination of $CaCO_3$ along with oxidation of Cu in the air reactor, given that the sorbent enters the air reactor in its carbonated form. If calcination is to be minimized, the air reactor must be operated at low temperature at atmospheric pressure, but must be pressurized if higher temperatures are required. One feature of Sequence 2 that might prove problematic is the circulation of Cu from the calciner to the carbonator on its way to the air reactor. The presence of copper in the pellet might not be trivial during the gasification stage, as copper is commonly used to catalyze the water-gas shift reaction at low temperatures (Gokhale et al., 2008) and might therefore contribute to enhancing the production of H_2. It should however be considered that while the water-gas shift reaction is exothermic and is therefore favoured at lower temperatures, the temperature in a biomass gasifier is considerably higher than in typical water-gas shift reactors which typically operate at 190°C-360°C (Ettouney et al., 1995). Beyond potential catalysis of the water-gas shift reaction, Cu serves no clear function in the gasifier and constitutes extra material required to transfer between different reactors; it essentially only requires to be circulated between the air reactor and the calciner. One way to circumvent this issue is to decouple the materials into separate Cu and limestone pellets and cycle them amongst the required reactors (gasifier and calciner for limestone-based pellets, air reactor and calciner for Cu-based pellets). This configuration, labelled as Sequence 3, is shown in Figure 1.9.

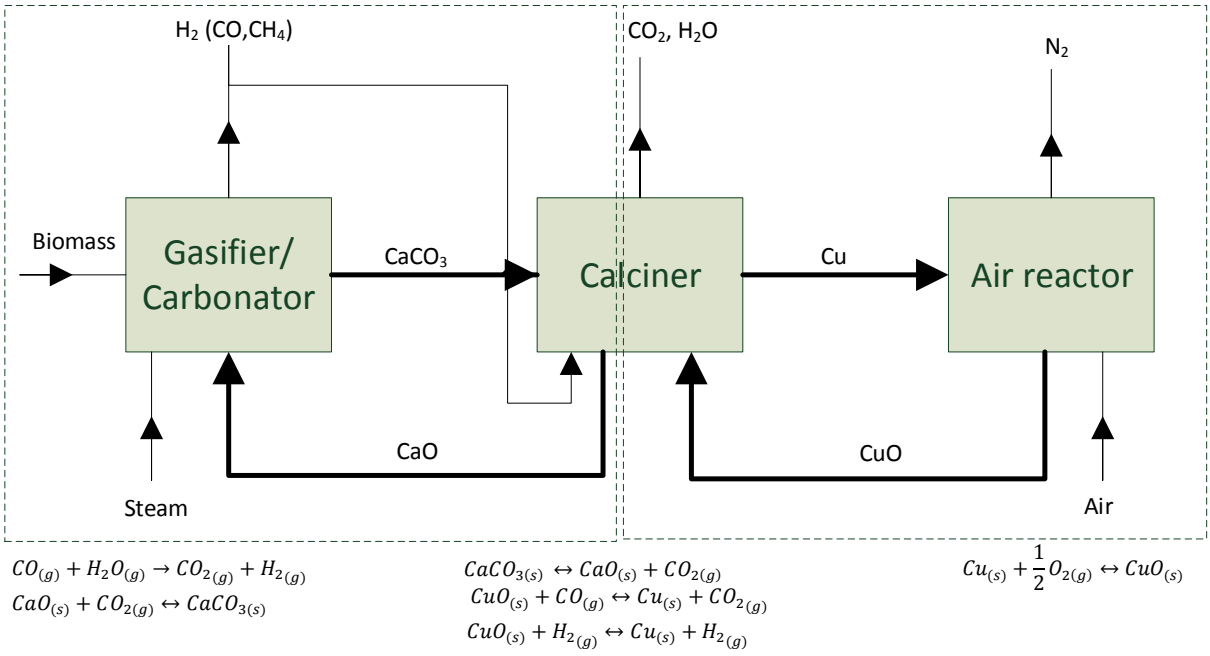

Figure 1.9 Sequence 3: reactor configuration upon decoupling of pellets into distinct Cu-based and limestone-based pellets

In contrast to Sequences 1 and 2, where the solids are circulated among all three reactors, Sequence 3 behaves as a dual-looping system where the Cu and limestone components only come into contact in the calciner. Beyond the added level of complexity of introducing two individual loops, given that limestone and Cu are not integrated within the same particle, the extent of contact between these two active species is less than in composite pellets, which could potentially lead to less effective heat transfer during reduction/calcination. Uncoupling the active CaO and CuO species into two separate pellets also means that a larger quantity of inert support might need to be employed relative to the composite pellets. The separation of the CaO and CuO-based pellets after regeneration in the calciner could also be a challenging task, even more so if the materials undergo agglomeration at the elevated temperatures involved. One important benefit of Sequence 3, however, is that it allows operating the air reactor at higher temperatures

than in Sequence 2 without the need for pressurization, as there is no concern of calcining any $CaCO_3$ within this configuration.

1.6 Thesis Objectives

The overall aim of this thesis was to investigate the integration of combined CaL-CLC with steam gasification of biomass through the utilization of composite pellets consisting of limestone, CuO and a calcium aluminate binder.

The specific objectives of the thesis were:

1. to determine the adequate sequence of solid circulation based on the extent of reduction of CuO within core-in-shell composite pellets during carbonation in the presence of syngas ($CO + H_2$);
2. to investigate the performance of composite CaO/CuO/alumina-containing cement pellets in the chosen reactor configuration (i.e., sequence) over multiple reduction-calcination-oxidation-carbonation cycles when the pellets are carbonated in different gaseous environments;
3. to determine how the Cu content in Cu/ alumina-containing cement pellets affects oxidation conversion and the pellets tendency to agglomerate when they are subjected to high temperature oxidation and reduction; and
4. to evaluate the carbonation conversion of limestone-based pellets when calcined at conditions relevant to the dual-looping process.

1.7 Thesis Outline

This thesis is composed of four chapters. Chapter 1 provides an introduction to the subject matter and explains the theory behind each of the major technologies being incorporated within the proposed process (biomass gasification, CaL and CLC). A brief review of the literature is also conducted, while potential challenges of the technology are also discussed.

Chapter 2 covers the information required prior to any collection of data. The materials and apparatus used are described, as well as the process through which the pellets are manufactured. Operation of the TGA and the conditions at which the runs are performed are established. The chapter also explains how to calculate the oxidation and carbonation conversions, a recurrent theme throughout the thesis.

Chapter 3 presents the results relating to the objectives established in Chapter 1. The relevant results, which include full TGA profiles, conversion profiles and particle characterization, are presented with accompanying discussion.

In Chapter 4, conclusions pertaining to the work presented in Chapter 3 are offered, and recommendations for future work are also suggested.

Chapter 2 Materials and Methods

In this chapter, all materials used to manufacture the composite pellets are described, as well as the apparatus used to test the pellets (namely the TGA). A brief procedure on the operation of the TGA is included, and calculations of carbonation and oxidation conversions are explained.

2.1 Materials

Composite pellets consist of CaO, CuO and a binder were prepared in-house. Powdered (<45 μm) Cadomin limestone (Alberta, Canada) was used as the source of CaO with its chemical composition, as determined through X-ray fluorescence (XRF) analysis, summarized in Table 2.1.

Fine CuO powder, with 98% of particles being < 5μm, supplied by Aldrich (USA) was used as the oxygen-carrier. A commercial calcium aluminate-based cement, CA-14 (71% Al_2O_3 and 28% CaO, with 80% of the particles <45 μm) produced by Almatis Inc. (Netherlands), was used as the binder.

The composition of the pellets varied for various experiments. The pellets were denoted by abbreviations corresponding to their components which were coupled with their relative mass fractions within the pellets. For example, Cu50-Ca40-Cem10 is a pellet composed of 50 wt% CuO, 40 wt% CaO and 10 wt% alumina-based cement.

Table 2.1 Chemical composition of Cadomin limestone

Component	Composition (wt. %)
SiO_2	2.25
Al_2O_3	0.61
Fe_2O_3	0.29
TiO_2	<0.03
P_2O_5	<0.03
CaO	51.36
MgO	2.31
SO_3	<0.10
Na_2O	<0.20
K_2O	0.22
Ba	<250 ppm
Sr	240 ppm
V	<50 ppm
Ni	<50 ppm
Mn	68 ppm
Cr	<50 ppm
Cu	<30 ppm
Zn	<30 ppm
Loss on Fusion (LOF)	42.92

The feed gases used throughout this work included nitrogen, carbon dioxide, compressed air and syngas supplied from gas cylinders. The syngas contained a pre-mixed mixture of 66% carbon monoxide and 34 % hydrogen.

2.1.1 Pelletization Procedure

A mechanical pelletizer (Glatt GmbH) was used to manufacture the pellets in a batch mode. Pellets could be produced according to two configurations: homogeneous or core-in-shell (see Figure 2.1). Core-in-shell pellets were similar to those used by Manovic et al. (2011) and consisted of a CuO-rich core coated with a layer of limestone mixed with calcium aluminate

cement, while homogeneous pellets were manufactured in such a way that the composition of the different components was largely uniform throughout the pellet. The aim of using core-in-shell pellets was to protect the more valuable and more toxic CuO material from attrition through the limestone/cement coating (Manovic et al., 2011).

To prepare homogeneous CuO/CaO pellets, a total of 300 g of pre-determined relative amounts of calcined limestone, CuO and binder were mixed in the pelletizer bowl. In the case of pellets prepared for operation in Sequence 3, CaO and CuO were uncoupled into homogeneous CaO-based pellets and CuO-based pellets respectively. Therefore, although the relative quantities of materials differed due to the different desired compositions, the overall procedure for the manufacture of homogenous pellets was left unchanged. Using compressed air,water droplets were sprayed onto the material through a nozzle while the material was mixed by a pair of rotor blades consisting of an agitator operating at 500 rpm fixed to the bottom of the vessel and a chopper operating at 2500 rpm on the side. The water droplets cause the formation of $Ca(OH)_2$ which has a sticking effect, leading the particles to agglomerate, but also to stick to the sides of the pelletizer bowl. As a result, the pelletizer was operated at 1 minute intervals, after which the material was scraped off the wall and the blades to ensure that all of the material, rather than just the hydrated part, would be in contact with the water droplets when the pelletizer operation was subsequently resumed. As more and more of the material became hydrated, the pelletizer operation time was gradually decreased from 1 minute to 5 seconds. When a desired particle size distribution (>200 μm) was deemed to have been reached, the chopper speed would be reduced to 800 rpm and the pelletizer was made to operate without any water. This particular step is the "shaping" stage and leads to the formed pellets to become more spherically shaped. Following

this step, the obtained pellets were sieved to the desired size range of 250 μm-600 μm, and dried. The size of the particles formed was principally a function of the time spent spraying the water droplets on the material (Manovic et al., 2011b)

The manufacture of core-in-shell pellets was carried out according to the same general principles as that of homogeneous pellets, but instead of having the different components all mixed simultaneously, the procedure required a two-stage pelletization process. The Cu-rich core was first prepared by mixing pre-calculated amounts of CuO and calcined lime. After a desired particle size distribution was attained, the cores were sieved to the desired size (~200μm) and immediately returned to the pelletization vessel, along with the required amounts of limestone and cement which constituted the shell. The coated CuO-enriched cores were retrieved and sieved to the required size (425-600 μm) and allowed to dry for 12 hours.

Core-in-shell pellets potentially suffer from multiple problems: not only their production is tedious and time-consuming, the final product is far from ideal with considerable amounts of copper (~20 wt.%) found in the shell as revealed by XRD analysis (Manovic et al., 2011) as well as the pellets dark color, as illustrated in Figure 2.1.

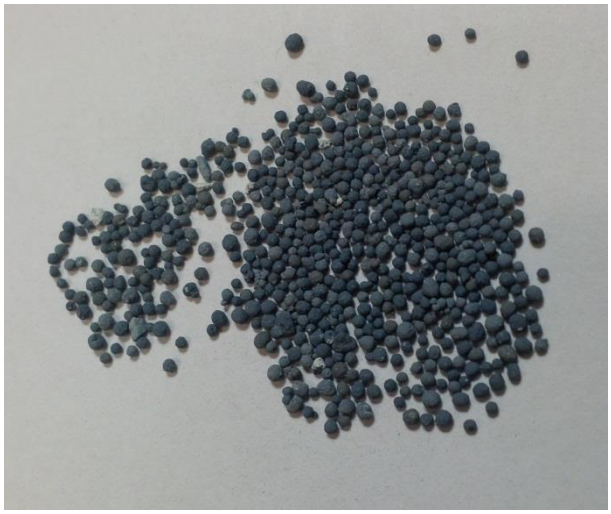

Figure 2.1 Core-in-shell Cu50-Ca40-Cem10 pellets

Moreover, some pellets were shown to have cracks at the core-shell interface and it is difficult to ascertain how those pellets would fare in realistic conditions when temperature changes are so fast that risks of thermal shock within the pellet cannot be ruled out. Core-in-shell pellets did not exhibit significantly higher attrition resistance than their homogeneous counterparts (Manovic et al., 2011). Furthermore, individual core-in-shell pellets can exhibit significant difference in composition; for example if CuO-based cores are sieved between 250-425 microns, and once the shell is formed the final product is sieved to a final particle size of 250-600 microns, it is quite conceivable that certain pellets would have a 250 microns core with a 350 microns shell, while others would possess a 425 microns core and a 175 microns shell. Whereas an overall composition can be better estimated for a whole batch of pellets (~300 g), this is not the case for small samples such as the ones used in a TGA.

2.2 Experimental Apparatus

Carbonation/oxidation/calcination-reduction cycles were carried out using a thermogravimetric analyzer system (TGA), illustrated in Figure 2.2.

A sample platinum pan (0.010 m in diameter) was suspended from a Cahn 1000 Electrobalance with 1 μg sensitivity and was nested within a cylindrical reactor column made of Inconel 625 alloy having an inner diameter of 0.025 m. A specific gas feed concentration was obtained by mixing various gasses (N_2, CO_2 and H_2/CO) supplied from cylinders at the inlet of the reactor. The flow rate of each gas was controlled by Brooks mass flow controllers. Steam was injected through the reactor using a 50 mL stainless steel syringe mounted on a Harvard PHD 440 syringe pump and steam generator. The lines carrying steam and mixed gases to the reactor column were equipped with electrical heat tracers and insulation to prevent condensation of steam. To maintain the balance at a moderate temperature and prevent its exposure to the feed gases, an inert purge gas (usually N_2) was fed from the top through the balance into the reactor column. The exiting gases were cooled and vented to the atmosphere.

Heat was supplied axially to the reactor column using a Lindberg Blue M 5.1 kW tube furnace, and K-type thermocouples strategically situated at the reactor inlet, sample pan, steam generator and reactor outlet allowed the monitoring of the temperature at those locations. The temperature of the furnace, gas flow rates and the output of the electrically heat traced lines were all controlled through the software interface. The sample weight measurements, temperatures and flow rates are recorded at pre-determined time intervals (typically 6 seconds).

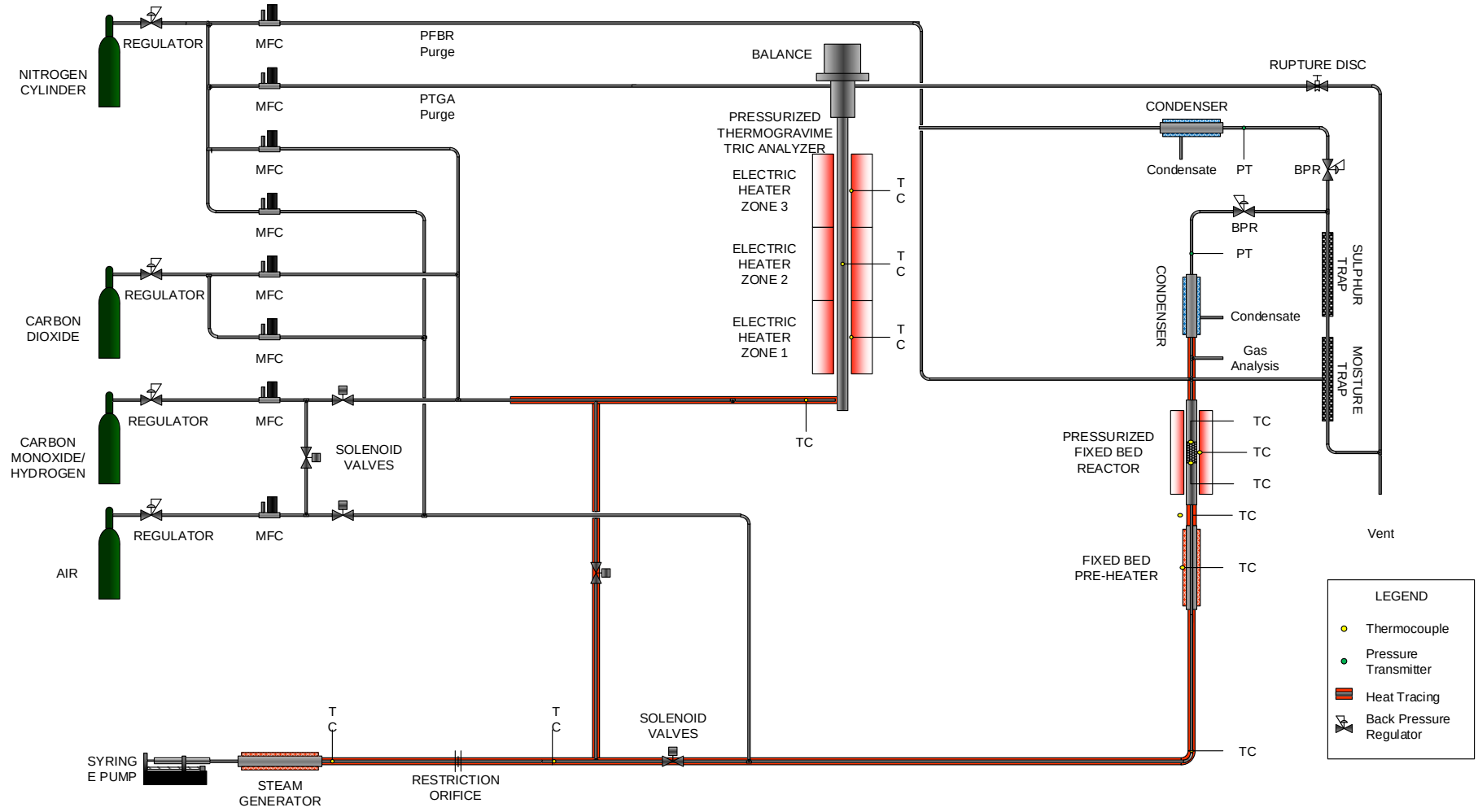

Figure 2.2 Schematic of the Thermogravimetric Analyzing System

A sample of about 25 mg of pellets was initially placed in the sample pan. While considering the initial mass of sample, using a generous amount of sample is preferable to minimize the effects of variance in chemical composition in individual pellets. The main consideration when choosing the sample mass was whether the amount used can provide a single layer of particles on the pan surface, avoiding any packing effect which could result in inter-particle mass transfer. The total gas flow rate fed to the reactor was maintained at 100 mL (STP)/min for all runs. The sample pan was loaded on a piece of platinum wire connected to the TGA balanced mechanism, and the reactor column was slowly mounted around the sample while ensuring not to hit the pan on the way up. The furnace was then fitted around the reactor column, and all lines were connected. Prior to starting the run, the heated steam line was intermittently purged from condensed steam and built up pressure. Such a precaution is essential, as a high buildup of pressure could knock the sample pan off the wire upon opening of the steam line valve. The gas cylinder valves were opened and the prepared recipe for the relevant run was loaded on the software interface. Once the recipe was loaded and activated, the system automatically carried out all the pre-determined steps listed within the recipe. The reproducibility of the experiments was ensured by carrying at least one repeat run for most of the tests performed.

In order to gain supplementary information and insight over the morphology of the materials used, BET (Brunauer-Emmett-Teller) and BJH (Barrett-Joyner-Halenda) analyses were carried out on some of the pellets. Since at least 1.5 g of material are required for nitrogen adsorption, it was not possible to carry out BET or BJH analyses of the samples at the end of the TGA runs due to the low amounts of materials involved. However, analyses of the freshly calcined materials were possible and gave valuable insight over their initial morphology. Nitrogen

adsorption measurements required for BET and BJH analyses were carried out using a Micromeritics TriStar II.

2.3 Sorbent Conversion

An example of results obtained from a typical multi-cycle carbonation-oxidation-calcination/reduction experiment using the TGA is illustrated in Figure 2.3. An enlarged view of the first cycle is provided in Figure 2.4 for a more detailed view of the sample mass changes during the various stages of each cycle. It can be observed that after each calcination stage, the sample weight does not drop back to the same previous baseline value, but actually appears to increase for the first 6 cycles before reaching a stable value, which is maintained until the end of the run. This phenomenon was systematically observed in every TGA run carried out and is not due to chemical changes in the sample, but is rather the result of buoyancy effects born from the gradual heating of the balance mechanism.

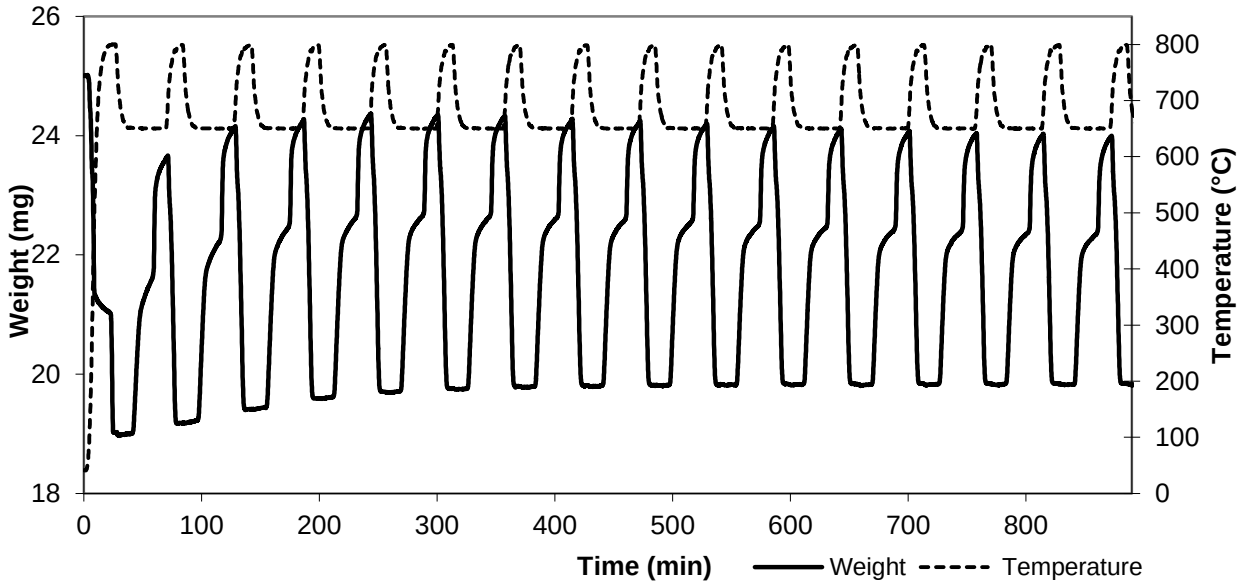

Figure 2.3 Multi-cycle carbonation-oxidation-calcination/reduction for 250-600 micron Cu50-Ca40-Cem10 pellets carbonated in 8% CO_2 and 92% N_2 using Sequence 2

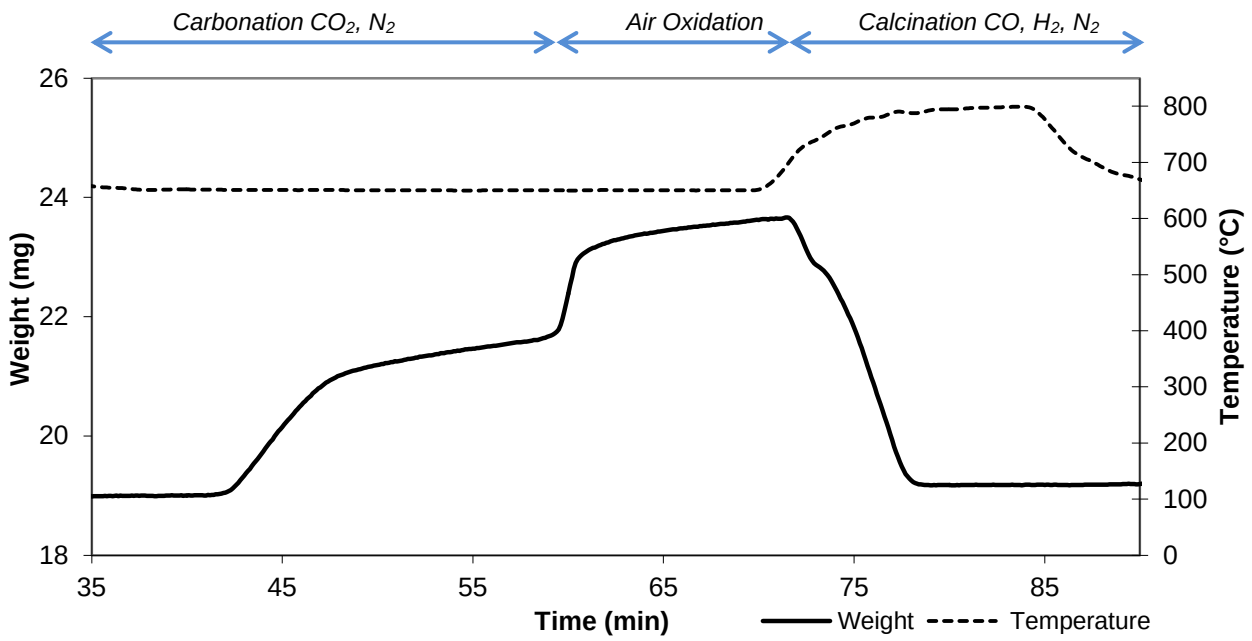

Figure 2.4 First cycle carbonation-oxidation-calcination/reduction for 250-600 micron Cu50-Ca40-Cem10 pellets carbonated in 8% CO_2 and 92% N_2 using Sequence 2

Equation (2.1) was applied to calculate the carbonation conversion, X_{Carb}:

$$X_{Carb} = \frac{m_{carb}(t) - m_{carb}(0)}{\left(\frac{MM_{CaCO_3}}{MM_{CaO}} - 1\right)\left(x_{CaO} \cdot m^0_{sample}\right)} \quad (2.1)$$

where $m_{carb}(t)$ is the mass of the sorbent at a time t after carbonation has begun, $m_{carb}(0)$ is the mass of the sorbent prior to the carbonation stage, MM_{CaCO_3} and MM_{CaO} are the molar masses of $CaCO_3$ and CaO respectively, x_{CaO} is the mass fraction of CaO in the pellet and m^0_{sample} is the mass of the calcined sorbent preceding the carbonation and oxidation stages. Quite similarly, the oxidation conversion of the Cu component within the sorbent, $X_{oxi,}$ was calculated through equation (2.2):

$$X_{Oxi} = \frac{m_{oxi}(t) - m_{oxi}(0)}{\left(\frac{MM_{CuO}}{MM_{Cu}} - 1\right)\left(x_{Cu} \cdot m^{0}_{sample}\right)} \tag{2.2}$$

where $m_{oxi}(t)$ is the mass of the sorbent at a time *t* from the onset of oxidation, $m_{oxi}(0)$ is the mass of the sorbent before the start of oxidation, MM_{CuO} and MM_{Cu} are the molar masses of CuO and Cu respectively, and x_{Cu} is the mass fraction of Cu in the pellet. While Cu_2O might also be involved in the process, there is no way of accurately estimating the fraction of Cu_2O formed based only on mass changes.

Chapter 3 Results and Discussion

This chapter presents the results of TGA experiments performed to evaluate the integrated CaL and CLC with biomass gasification while CaO-CuO based sorbents were used. The solids circulation sequence through which the different operations of calcination, carbonation and oxidation needed to be carried out was first identified. Subsequently, the effect of the carbonation gas feed composition on the carbonation and oxidation conversions over multiple cycles was evaluated in the chosen sequence. Finally, in view of simulating a dual-loop process, the performances of CuO-based pellets and CaO-based pellets were evaluated individually within their respective CLC and CaL loops, where the Cu content and calcination conditions were varied.

3.1 Sequence of Solids Circulation for Composite Pellets

The present section aims at evaluating Sequence 1 as a possible configuration for integration of combined CaL-CLC with steam gasification of biomass. Sequence 1 may only be used in such a scenario if CuO can be maintained in its oxidized state in the gasifier (carbonator). In order to determine whether the CuO present in the pellet undergoes significant reduction even at low residence times when the pellet is exposed to a mixture of CO_2, CO and H_2, a simple experiment was designed based on sequence 1 using 425-600 micron core-in-shell Cu50-Ca40-Cem10 pellets. The use of core-in-shell pellets is warranted in the present case because it was speculated that access to the CuO core may become increasingly limited as the CaO shell is being carbonated. The composition of the pellet was determined by taking into account the stoichiometries and enthalpies of reactions (1.10) and (1.12) and considering that the amount of heat released by the reduction of CuO in methane that would be sufficient to calcine the $CaCO_3$

formed if the CaO conversion prior to calcination was about 30% (Manovic et al., 2011a). Such a conversion is chosen because CaO is never completely carbonated by CO_2, and assuming 100% carbonation would lead to a much higher Cu content within the pellet. This could potentially have a long-term detrimental effect given that, as the CaO conversion declines, the heat provided by the CuO reduction would become in excess of what is actually required to calcine the lower quantity of $CaCO_3$ formed. Although the syngas mixture (66% CO, 34% H_2) used during the calcination/reduction step would in a real-life system release an amount of heat in excess of that released by reduction by methane, this is not an issue in the present system as the heat is primarily supplied by the furnace.

The pellets were initially calcined in pure N_2 at 800°C, leaving the pellets in the form of CaO-CuO-Al_2O_3-based cement. The sample was then subjected to a carbonation stage in a gaseous environment composed of 8% CO_2, 22% CO, 11% H_2 and balance N_2 at 650°C for 4 minutes. This time duration was chosen because it was low enough to loosely simulate a low-residence time carbonation stage, but high enough for the gas flow rate to reach a quasi-steady state between the mass flow controllers and the sample in the reactor. The pellets were subsequently calcined in pure N_2 again at 800°C. The result of the experiment is presented in Figure 3.1. Since calcination in pure N_2 at 800°C should not have any effect on CuO, any difference between the sample weight after the initial and final calcinations must be due to reduction of CuO during the carbonation stage.

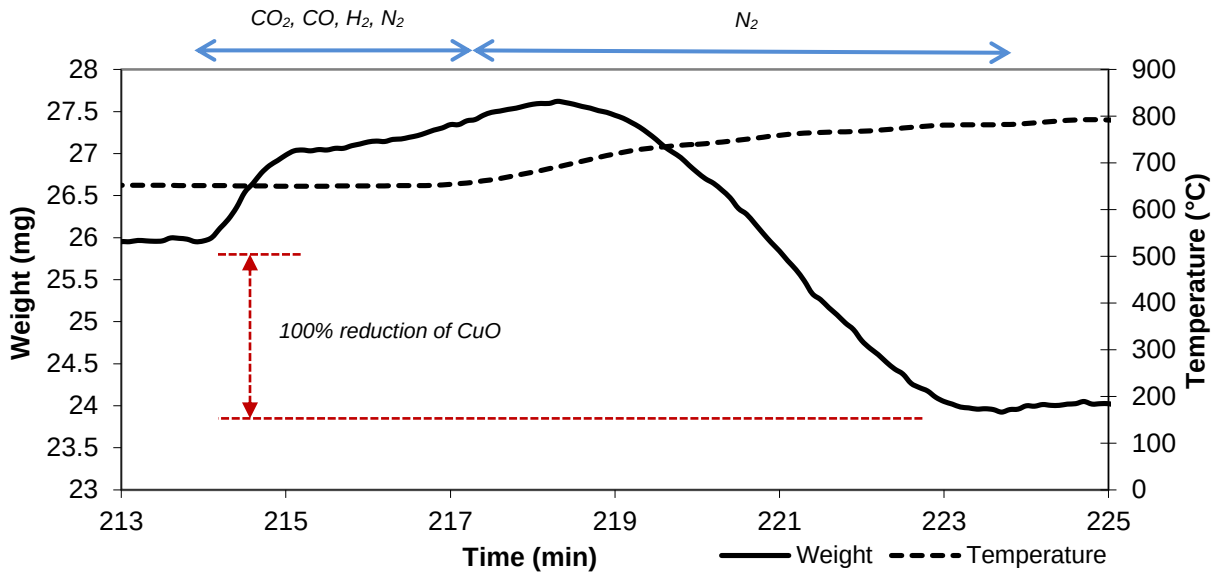

Figure 3.1 Carbonation of core-in-shell Cu50-Ca40-Cem10 pellets in the presence of CO and H_2

As can be seen in Figure 3.1, before the onset of the carbonation stage, the sample weighs 25.95 mg. However, following the carbonation, the sample is calcined, which drives the weight to drop to 23.93 mg. If this difference in mass is accounted for on the basis of CuO reduction, calculations show that practically 100% of the CuO available has been reduced to Cu. This result demonstrates that even as CaO is being carbonated to $CaCO_3$ in parallel within the shell of the pellet, H_2 and CO molecules are still able to access the CuO-rich core and completely reduce the CuO within 4 minutes of carbonation stage. The kinetics of CuO reduction are thus quite rapid with the relatively small-sized H_2 and CO molecules being able to diffuse through the porous CaO and then the "non-porous" $CaCO_3$ layer formed, to reach the CuO grains.

The obtained result represents a strong indication that the Sequence 1 (Figure 1.7) involving the solids to be transferred from the gasifier directly to the calciner is not a viable option. While the use of core-in-shell pellets is justifiable in the context of experiment presented in Section 3.1, subsequent experiments were carried out using homogeneous pellets.

3.2 Effect of Carbonation Feed Composition

The ability of Cu50-Ca40-Cem10 pellets to sustain high carbonation and oxidation reactivity over multiple cycles at various carbonation feed compositions were investigated. Given the elimination of Sequence 1 for the proposed process, composite Cu-Ca-Cem pellets hereon were tested through Sequence 2. While the use of CuO and CaO pellet for combined chemical looping combustion-calcium looping has been reported by different authors (Imtiaz et al., 2012; Qin et al., 2012), the results were always reported for the configuration involving oxidation of Cu prior to carbonation of CaO (Sequence 1). It appears that existing literature does not contain any reported experimental data with regards to the other configuration involving carbonation of CaO followed by oxidation of Cu (Sequence 2). While experiments performed so far using Sequence 1 have generally confirmed the high reactivity of the Cu portion of the sorbents used, it is still unclear how carbonating the latter prior to oxidation will affect the oxidation conversion.

Experiments were conducted with homogeneous 250-600 micron Cu50-Ca40-Cem10 pellets, where multiple cycles of carbonation, oxidation and calcination/reduction (Sequence 2) were performed. Carbonation was carried out at 650°C for 20 min under different gaseous environments, which along with the other test conditions are summarized in Table 3.1

Table 3.1 Test conditions for the carbonation, oxidation and calcination-reduction stages used with Sequence 2.

	Carbonation	**Oxidation**	**Calcination-Reduction**
Temperature (°C)	650	650	800
Duration (min)	20	10	10
Gas Composition (Vol. %)	8% CO_2, 92% N_2	Air	20% CO, 10% H_2, 70% N_2
	8% CO_2, 22% CO, 11% H_2, 59% N_2		
	8% CO_2, 22% CO, 11% H_2, 20% H_2O, 39% N_2		

A CO_2 concentration of 8% was kept constant for carbonation throughout all the tests carried out, with the balance consisting of varying amounts of CO, H_2, H_2O and N_2. The different compositions used during the carbonation stage correspond to carbonation in the absence of syngas (CO_2 and balance N_2 only), carbonation with dry syngas (CO_2, CO, H_2 and balance N_2) and carbonation with wet syngas (CO_2, CO, H_2, H_2O and balance N_2). Testing with dry syngas and wet syngas was essentially the equivalent of testing for the presence of steam, an important variable given its enhancing effect on carbonation conversion (Dou et al., 2010; Manovic & Anthony, 2010b; Yang & Xiao, 2008) and its role in the water-gas shift reaction (Symonds et al., 2009). Diluting the simulated syngas (CO and H_2) with N_2 during the calcination step was necessary since at high concentrations of CO, significant carbon deposits formed on the inner surface of the column, as can be seen in Figure 3.2.

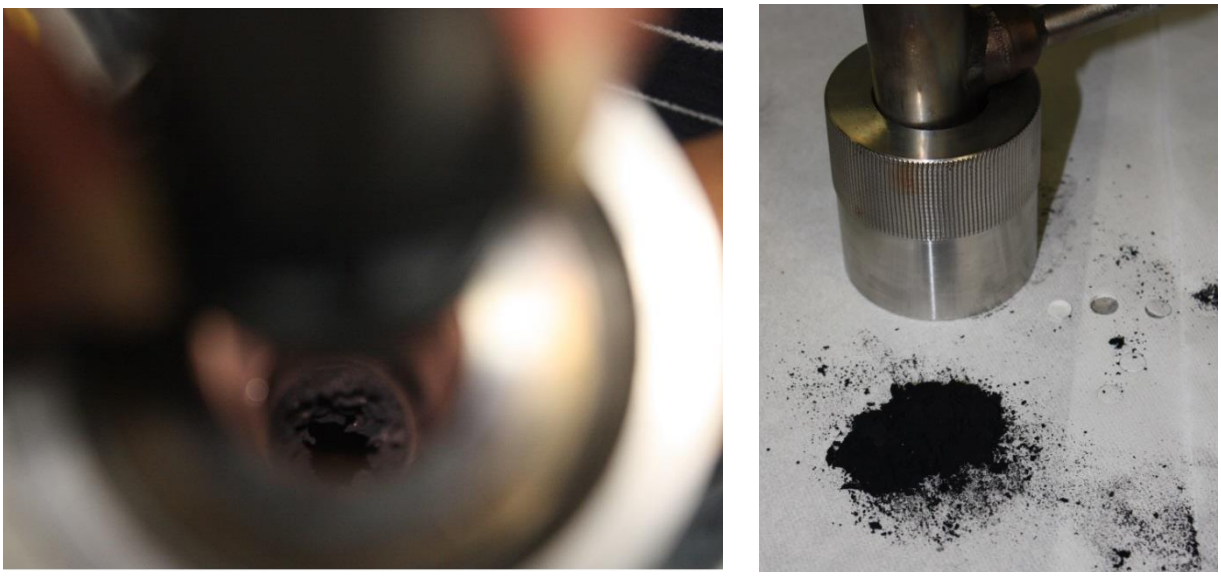

Figure 3.2 Carbon deposits formed on the inner sides of the reactor column as a result of "metal dusting"

This phenomenon was observed after preliminary runs using 100 mL (STP)/min of simulated syngas were carried out, but was considerably reduced when the flow rate of syngas in subsequent runs was reduced to 30 mL (STP)/min while diluted with 70 mL (STP)/min of N_2. This phenomenon, known as "metal dusting", is common in processes involving metal alloys and high carbon activity in the gaseous atmosphere that leads to corrosion of the metal surface as well as formation of graphite (Grabke et al. 1996). Between the carbonation, oxidation and calcination stages, the reactor column was purged using N_2 in order to avoid mixing of oxygen with combustible CO and H_2.

Figure 3.3 shows the carbonation conversions results of the homogeneous Cu50-Ca40-Cem10 pellets when carbonated under different gaseous environments. Irrespective of the carbonation conditions, the sorbent experienced a reduction in carbonation conversion with the number of cycles, a trend which is typical of CaO-based sorbents. Carbonating together with either CO/H_2 or CO/H_2/steam resulted in higher overall carbonation conversions than with CO_2 only. The water-gas shift reaction, shown in equation (1.2), has been reported to be catalyzed by CaO sites (Symonds et al., 2009). As CO_2 reacts with CaO, disturbing the system's equilibrium, the system adjusts as predicted by Le Chatelier's principle by shifting the equilibrium to the products side, producing more H_2 and CO_2 to compensate for the disturbance. This results in increased local CO_2 concentrations in and around the pellets, yielding enhanced carbonation kinetics. It is also possible that the water-gas shift reaction takes place upstream of the sample, which then comes into contact with a higher CO_2 concentration than the predicted 8%.

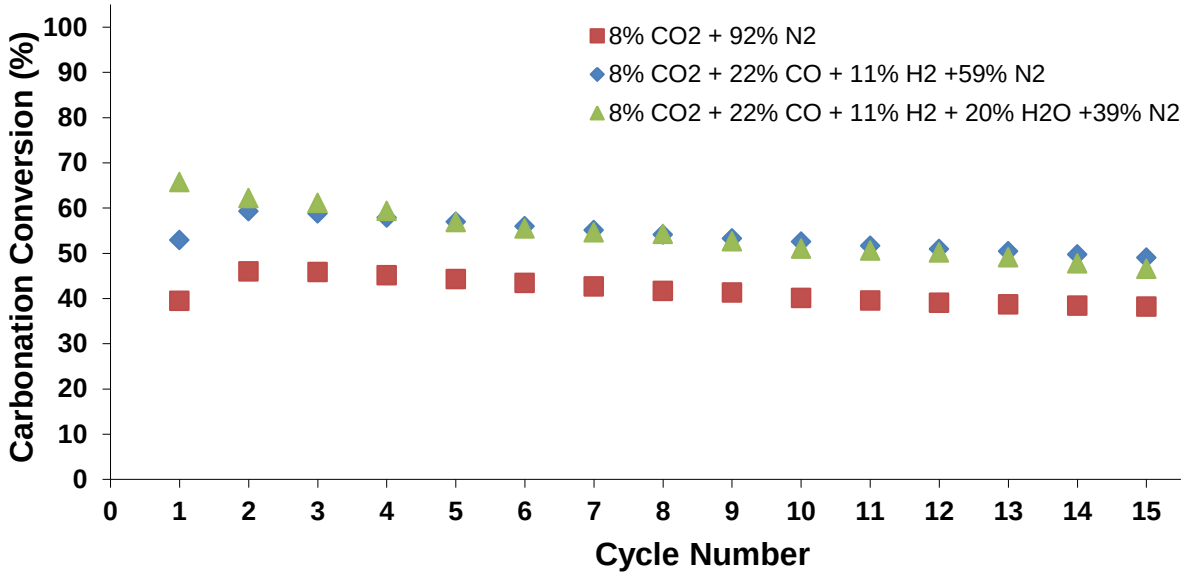

Figure 3.3 Carbonation conversion of homogeneous Cu50-Ca40-Cem10 pellets when subjected to different carbonation gaseous environments

It is to be noted that CO, H_2 and H_2O molecules are all considerably lighter than CO_2 molecules. While the latter might experience some difficulty accessing the CaO grains covered by the formed $CaCO_3$ layer, CO, H_2 and H_2O molecules are more likely to permeate through the latter given their inherently higher mass diffusivity. The enhancement of carbonation in the presence of steam is a well-documented phenomenon, which has been accounted for on the basis of $Ca(OH)_2$ formation (Dou et al., 2010), steam catalysis of the CaO-CO_2 reaction (Yang & Xiao, 2008) and amplified solid-state diffusion (Manovic & Anthony, 2010).

It can be seen that for some of the runs, the carbonation conversion appears to increase from the first to the second cycle and then declines throughout the following 13 cycles. Two main explanations can be offered for this phenomenon. The first possible explanation is that the pellets are undergoing "self-reactivation", a phenomenon where CaO-based sorbents experience a temporary increase in reactivity. The term was coined by (Manovic & Anthony, 2010a) when

they made similar observations following tests carried out on limestone. The authors showed that the number of cycles over which self-reactivation takes place is dependent on the sorbent used, with powdered limestone thermally pre-treated at 1000°C experiencing self-reactivation throughout the 30 tested cycles. Given that composite Cu50-Ca40-Cem 10 pellets are being used in the present study rather than limestone, the very short period over which "self-reactivation" is suspected to occur in could therefore be attributed to the radically different nature of the material used.

The second possible explanation relates to the operational procedure. Given that a significant portion of the runs performed on the TGA required steam, the lines contained a considerable amount of condensed steam after the completion of the runs. Although part of steam line can be preheated and purged from any condensate prior to a new run, this does not extend to all the lines. As a result, a portion of the line upstream of the sample may still contain condensed steam at the beginning of the run, which would impede the flow of the gas to the sample. This would reduce the amount of CO_2 present in the reactor column contacting the sample. It is plausible that as the run proceeds and the system heats up, the water in the line evaporates, clearing the line such that by the second cycle the incoming gases flow unobstructed.

In addition to carbonation of CaO and the water-gas shift reaction, another reaction likely to take place in presence of CO is the Boudouard reaction, illustrated in equation (3.1).

$$2CO \leftrightarrow C + CO_2 \qquad \Delta H^r_{650^\circ C} = -171.4\, kJ/mol \tag{3.1}$$

While the formation of carbon deposits was not visually apparent on the sample itself given the sample black color, a thin black layer was consistently observed on the inner surface of the reaction column after experimental runs with syngas. The Boudouard reaction being exothermic, is favored at lower temperatures and is therefore less likely to take place at the relatively high calcination temperature of 800°C. The same cannot be said for the carbonation temperature of 650°C. Similarly to the water-gas shift reaction, the consumption of CO_2 would result in an equilibrium shift towards the right side of the reaction, causing increased local concentrations of CO_2, which could explain the higher conversions obtained compared to the case when the sample is carbonated under only CO_2 and N_2. Due to the presence of nickel in the metal alloy from which the reactor column is made of, the Boudouard reaction is easily catalyzed on the inner surface of the tube, generating a higher CO_2 content in the main gas stream contacting the sample. Interestingly, while it would be expected that the presence of steam would yield overall higher carbonation conversion, the carbonation conversions in the presence of simulated syngas, with or without steam, were very similar. It needs to be pointed out, however, that if the Boudouard reaction is taking place in the vicinity of the CaO grains, carbon might be deposited at those locations, leading to additional mass increase during the carbonation stage which, if factored in, can in part account for the seemingly enhanced carbonation conversion. Such a phenomenon was observed by Manovic & Anthony (2011a) while conducting experiments with Cu45-Cu45-Cem10 pellets using syngas as calcination medium.

The oxidation conversation results of the sorbent are presented in Figure 3.4. It can be seen that the sorbent experienced a drop in oxidation conversion for all the conditions tested, a stark contrast to what has been presented in the literature (Imtiaz, et al., 2012; Qin et al., 2013). It also

appears that oxygen-carrying capacity is quite dependent on the carbonation conditions employed prior to oxidation; while the oxidation conversion plateaus to the relatively high value of 77 % when the sample is carbonated in CO_2 and N_2 only, it undergoes dramatic decay when carbonation is performed in CO/H_2 and CO/H_2/steam environment, plateauing at around 26 % and 10 %, respectively.

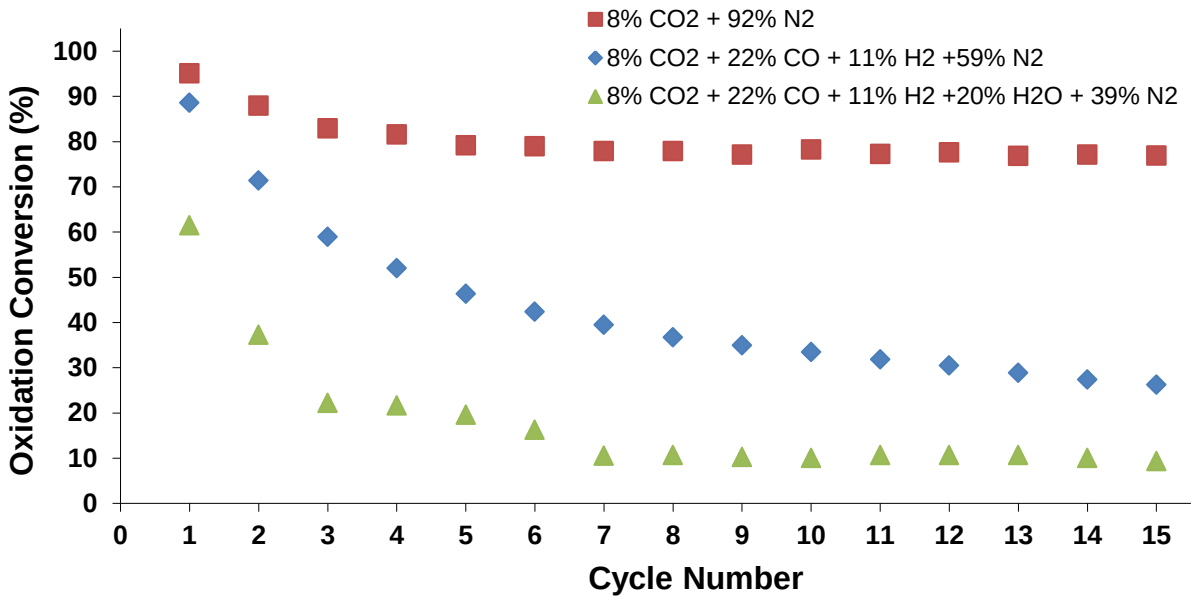

Figure 3.4 Oxidation conversion of homogeneous Cu50-Ca40-Cem10 pellets following carbonation in different carbonation gaseous environments

In order to determine the reasons for such variation in results, the test involving carbonation in the presence of simulated syngas in the absence of steam was repeated using approximately 100 mg of initial sample. This testing was conducted in order to collect enough sample for X-ray diffraction (XRD) characterization, which was carried out after the 15th cycle, following the final oxidation step. The XRD spectra obtained is presented in Figure 3.5 while the chemical compositions are summarized in Table 3.2.

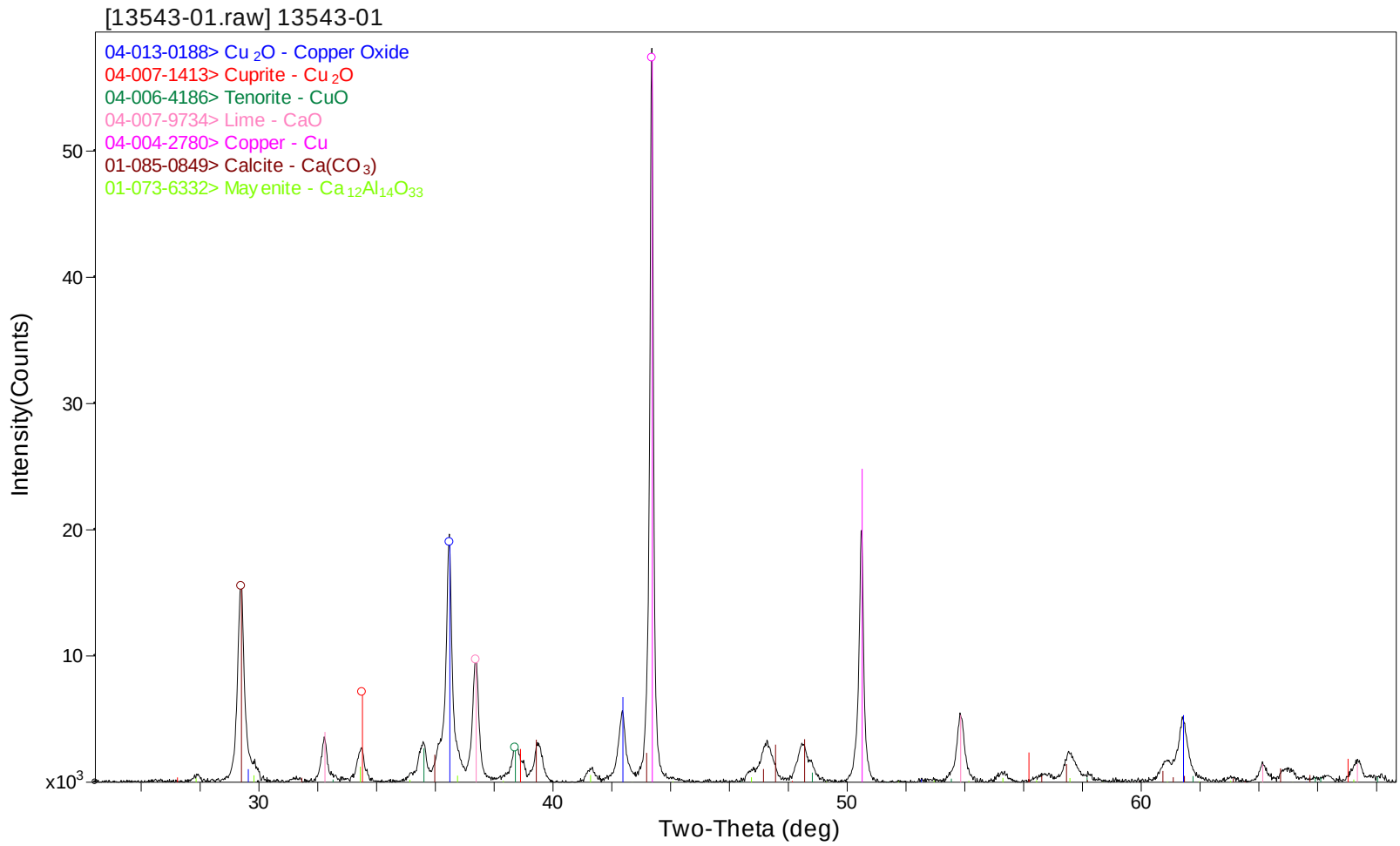

Figure 3.5 XRD spectra of Cu50-Ca40-Cem10 pellets after 15 cycles of carbonation in 8% CO_2, 22% CO, 11 % H_2 and 59% N_2 and oxidation

Table 3.2 Chemical composition of Cu50-Ca40-Cem10 pellets determined from XRD data after 15 cycles of carbonation in 8% CO_2, 22% CO, 11 % H_2 and 59% N_2 and oxidation

Chemical compound	**Chemical Formula**	**wt %**
Copper Oxide	Cu_2O	11.0
Cuprite	Cu_2O	1.0
Tenorite	CuO	6.9
Lime	CaO	10.8
Copper	Cu	25.9
Calcite	$Ca(CO_3)$	23.3
Mayenite	$Ca_{12}Al_{14}O_{33}$	3.6
Crystallinity (wt. %)		82.4
Amorphous (wt. %)		17.6

The XRD analysis results are consistent with the results obtained through the experiments performed using the TGA, in the sense that after the 15th oxidation step, only a small quantity of the Cu in the sample is found to be present in its most oxidized form (CuO). This confirms the low oxidation conversion determined as per the TGA experiments. An analysis of the chemical composition of the sample yields valuable insight that cannot be obtained solely through thermogravimetry. Even after being exposed to air at 650°C for 10 min, most of the Cu was found to be in its reduced, metallic form. This implies that Cu was not reacting completely with O_2, suggesting that diffusional aspects may have become important at this point. Only 3.6 % of mayenite ($Ca_{12}Al_{14}O_{33}$) was detected, far less than would be expected considering that 10% of calcium aluminate cement could potentially lead to a maximum mayenite content of 20% upon reaction of CaO with Al_2O_3 (Manovic and Anthony 2009a). The significant amount of copper oxide within the pellet appears to limit the degree of contact between calcium oxide and the alumina within the cement binder, which would account for the noticeably small amount of mayenite formed. It is also interesting to note that while mayenite was formed, no copper aluminate, either in the form of $CuAlO_2$, or $CuAl_2O_4$ was detected.

Further testing was performed to assess whether the copper oxidation decline was the result of Cu becoming increasingly chemically inactive (possibly due to sintering) or simply having its access to oxygen molecules restricted because of the $CaCO_3$ product layer formed around it. In this experiment, after completing 15 cycles where the sorbent was carbonated in 8% CO_2 (balance N_2), oxidized in air at 650°C, and calcined at 850°C, a subsequent oxidation step was conducted. This meant that at the onset of oxidation, the pellet was in the form of CaO-Cu-Al_2O_3-based cement in the absence of any $CaCO_3$ product layer. The results of this run are presented in Figure 3.6

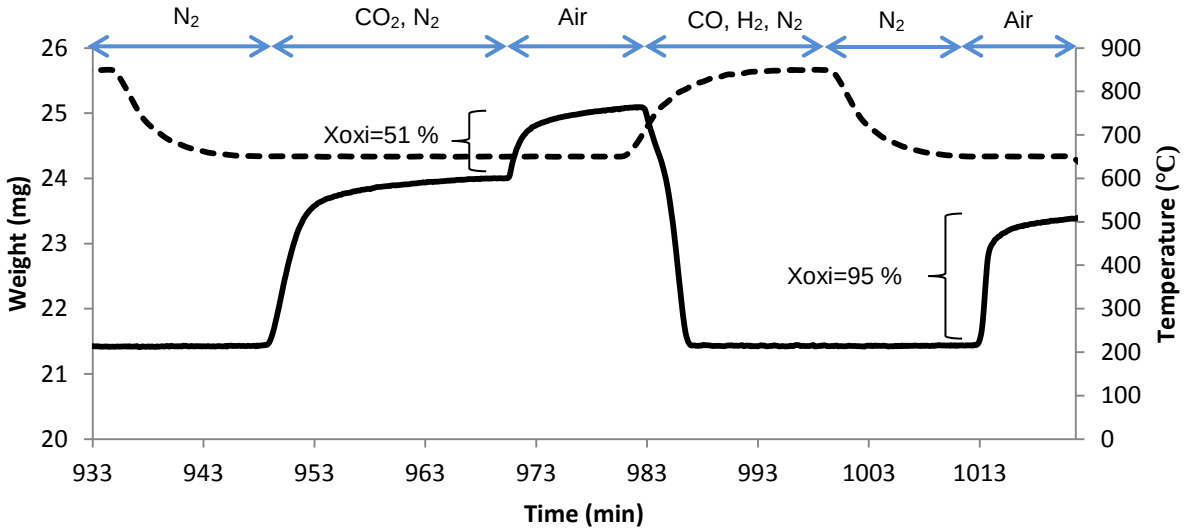

Figure 3.6 The 15th carbonation/oxidation/calcination/reduction cycle of Cu50-Ca40-Cem10 pellets followed by an oxidation step

It is apparent from the results that oxidation of the pellet in its non-carbonated form was significantly higher than in its pre-carbonated form. While the oxidation conversion of the sample amounted to only 51 % for the 15th carbonation-oxidation-calcination/reduction cycle, subsequent oxidation of the pellet in its reduced form resulted in a 95 % conversion. This

indicates that even after 15 cycles, the decline in oxidation conversion was not due to Cu being irremediably chemically deactivated, but was indeed intrinsically connected to the carbonation taking place prior to the oxidation stage. It appears that the formation of a low porosity $CaCO_3$ product layer provides a considerable resistance for O_2 molecules to diffuse through to the Cu grains. Sun et al. (2007) showed through mercury intrusion that carbonated limestone did not present any pore volume as a result of pore blockage, which confirms that carbonation results in a highly non-porous material. This can also explain the correlation between higher carbonation conversion and lower oxidation conversion; the more the pellet is carbonated, the more difficult it is for oxygen molecules to subsequently access the inner Cu sites within the particle.

Results also indicated that presence of steam reduces the oxidation conversion. Although the presence of steam does not appear to affect the kinetics of carbonation during the reaction-limited stage, it has been shown to considerably affect the rate of carbonation during the diffusion-limited regime (Arias et al., 2012). In the presence of steam, accelerated solid-state diffusion of CO_2 through the product layer to the inner CaO sites leads to more of the CaO being carbonated to $CaCO_3$. Considering that $CaCO_3$ also occupies more space than CaO, O_2 molecules are faced with an even less-porous material than in the absence of steam on their way to react with Cu. This confirms the results presented in Figure 3.4. Moreover, if Cu indeed catalyzes the water-gas shift reaction at the carbonation temperature involved, the increased local CO_2 concentration in the vicinity of the Cu grains may lead to adjacent CaO grains being preferentially carbonated, which would mitigate access of those specific grains to O_2 molecules, and hence also account for the drastic loss in oxidation conversion.

The non-static morphological nature of the pellets can also be a contributing factor in the decreasing oxidation conversion of Cu. Sun et al. (2007) showed that the pore size distribution of

limestone changed significantly with increasing number of calcination cycles while Manovic et al. (2009) demonstrated that carbonation/calcination cycles led to particle densification. As the carbonation conversion of Cu50-Ca40-Cem10 pellets decreases with the number of cycles, presumably as a result of sintering effects, the resulting shift in porosity and particle shrinkage potentially lead to more compact pellets, further limiting the mobility of O_2 molecules through the material. Contrary to core-in-shell pellets, homogeneous composite pellets always have some Cu sites at the surface of the pellets which are likely to be oxidized, and therefore partial oxidation is expected. Although no significant loss in oxidation conversion has been observed in works presented in literature for similar processes, it is to be noted, that the main difference lies in the sorbent being carbonated prior to the oxidation of Cu as in the current configuration, the reverse sequence of what has been traditionally performed to this point (i.e. Sequence 1). The oxidation conversion can be sustained at close to 100% for Sequence 1 because the material is oxidized while in its calcined state, and is at that specific point more porous than if it was in its carbonated form. Even if the sorbent in Sequence 1 experienced cyclic particle densification, the fact that it is oxidized while in its calcined state should make it porous enough to achieve excellent oxidation conversion. Oxidizing the pellets prior to carbonation does not appear to have significant adverse effects on the carbonation conversion because CuO (molar volume 12.4 cm^3/mol) does not occupy significantly more space than Cu (molar volume 7.11 cm^3/mol). For every mole of Cu oxidized, only about 5.3 cm^3 of new material is formed within the porous framework of the pellet, compared to 20 cm^3 per mole of CaO carbonated, a significant difference.

The BET surface area of Cu50-Ca40-Cem10 pellets was determined to be 2.97 m^2/g, a relatively low value consistent with those found in literature for similar materials. Manovic & Anthony

(2011b) reported the surface area of 1.0 mm diameter Cu45-Ca45-Cem10 pellets to be 1.69 m^2/g , whereas Kierzkowska & Müller's (2012) co-precipitated CuO-CaO sorbents exhibited surface areas of 2.81 m^2/g, 4.28 m^2/g and 3.80 m^2/g for CuO to CaO ratios of 1:1, 1.3:1, and 3.3:1, respectively. While the BET surface area of limestone-based pellets has been reported to be quite high (Manovic & Anthony, 2009b), CuO is a low porosity material which even when combined with limestone and calcium aluminate cement appears to result in a relatively low-porosity product. This is problematic in the current system; the BET surface area is determined for the calcined material, and it is very likely that carbonation of the CaO component within the pellet further reduces the available surface area and porosity of the pellet before the onset of oxidation.

3.2.1 Uncoupled Pellets

If indeed the formation of $CaCO_3$ and its plugging of pores are the cause for the reduced oxidation conversion in composite pellets, it stands to reason that uncoupling Cu and CaO in two separate pellets and their subsequent testing under similar conditions should lead to a more sustained oxidation conversion. The rationale behind this assumption is that with no carbonation taking place within a Cu/Al_2O_3-containing cement-based pellet, oxygen molecules should encounter significantly less diffusional resistance on their way to react with Cu as opposed to the composite pellets.

In order to test this hypothesis, an experiment involving Cu and CaO separated in two distinct homogeneous pellets (Cu80-Cem20 and Ca90-Cem10) was carried out. A mixture of the two pellets was prepared by using 36.5 mg of Cu80-Cem20 pellets and 26.0 mg of Ca90-Cem10 pellets. Those masses were pre-determined in order to keep the Ca/Cu ratio the same as in the

composite pellets used so far (Ca/Cu=0.45). The CuO-pellet composition (80% CuO supported with 20% cement) was chosen because a Cu content any lower would require a too high amount of CuO pellets to maintain the Ca/Cu ratio at 0.45. Conversely, a higher CuO content could lead to significant agglomeration and sintering, causing a decline in the oxidation conversion. The composition of Ca90-Cem10 pellets was chosen based on work conducted by Manovic & Anthony (2009a) which established a binder content of 10% as optimal based on performance and costs. The test conditions are summarized in Table 3.3.

The TGA profile obtained for the 15 cycles is shown in Figure 3.7, while the carbonation and oxidation conversions are shown in Figure 3.8.

Table 3.3 Summary of test conditions for uncoupled Cu and limestone-based pellets

	Carbonation	**Oxidation**	**Calcination-Reduction**
Temperature (°C)	650	650	800
Duration (min)	20	10	10
Gas Composition (Vol. %)	8% CO_2, 22% CO, 11% H_2, 59% N_2	Air	20% CO, 10% H_2, 70% N_2
Mass of Cu80-Cem20 pellets (mg)	36.5		
Mass of Ca90-Cem10 pellets (mg)	26.0		
Particle Size Range (µm)	250-600		

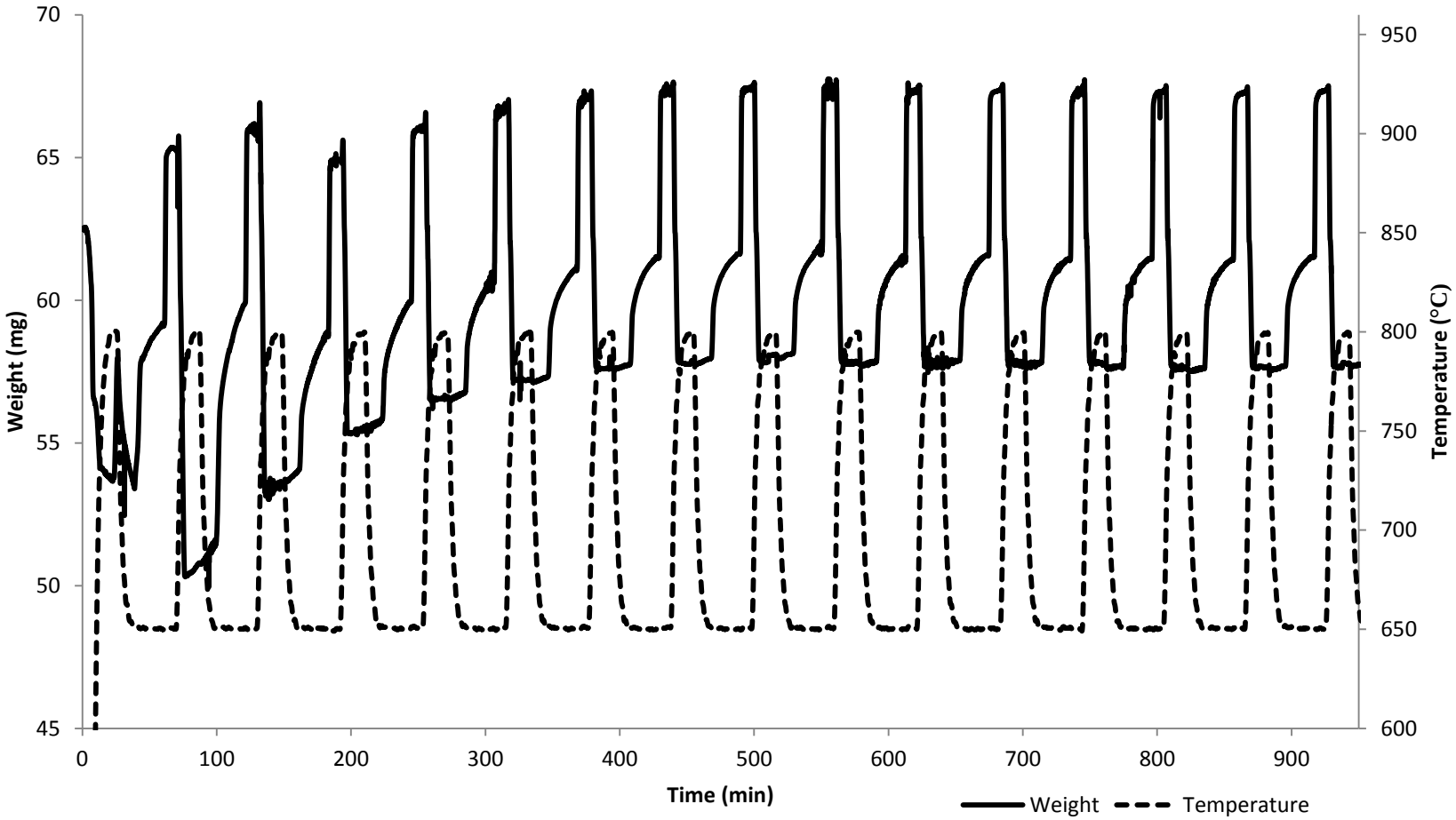

Figure 3.7 TGA profile for carbonation-oxidation-calcination-reduction cycles for Cu80-Cem20 pellets mixed with Ca90-Cem10 pellets carbonated in 8% CO2, 22% CO, 11 % H_2 and 59% N_2

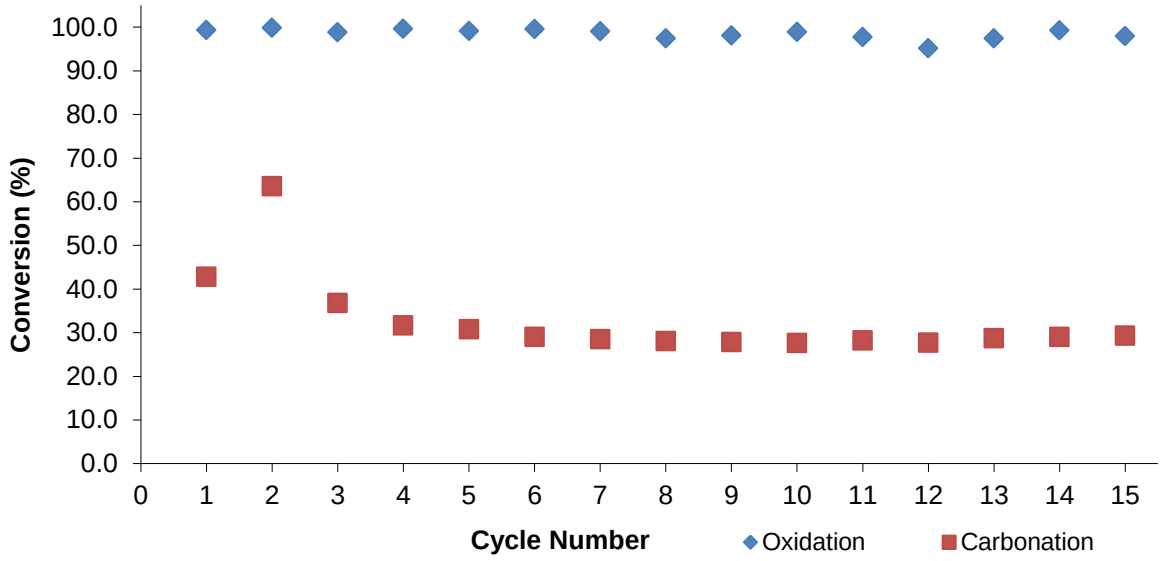

Figure 3.8 Carbonation conversion of Ca90-Cem10 pellets and oxidation conversion of Cu80-Cem20 pellets

Compared to composite Cu50-Ca40-Cem10 pellets tested under identical conditions, Cu80-Cem20 pellets barely experienced any decrease in oxidation conversion throughout all 15 cycles. Ca90-Cem10 pellets, on the other hand, exhibited a lower carbonation conversion than expected, with the 15th cycle carbonation conversion amounting to only 29.3 %, compared to 50 % for Cu50-Ca40-Cem10 pellets. This significant difference can be attributed to the amount of sample used; in order to have enough of both Ca90-Cem10 and Cu80-Cem20 pellets and ensure homogeneity in the composition of active species, a total sample mass of 62.5 mg was used, such that instead of the usual monolayer of particles usually employed, the quantity used resulted in the generation of multiple layers of pellets which in turn led to a "packing effect" within the sample pan, sheltering some of the Ca90-Cem10 pellets from CO_2. The first cycle oxidation

conversion with time profile for Cu50-Ca40-Cem10 composite pellets and Cu80-Cem20 uncoupled pellets are presented in Figure 3.9.

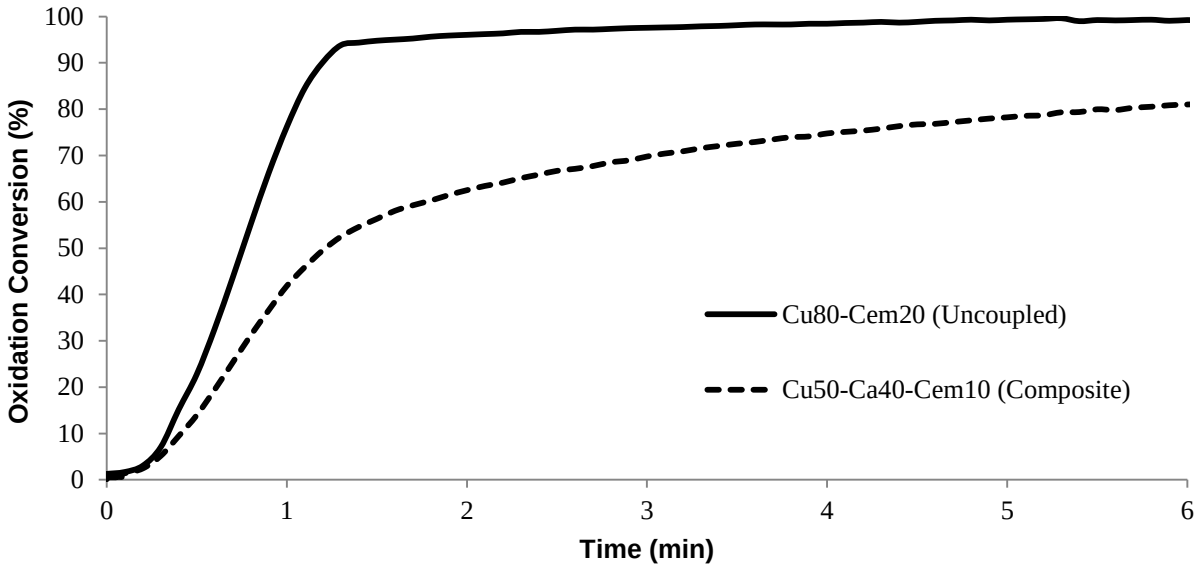

Figure 3.9 First oxidation stage for Cu80-Cem20 uncoupled pellets and Cu50-Ca40-Cem10 composite pellets following carbonation in 8% CO_2, 22% CO, 11 % H_2 and 59% N_2

It can be observed that the slope of the curve is steeper in the case of Cu80-Cem20 pellets at all points, suggesting overall faster kinetics than during the use of Cu50-Ca40-Cem10 pellets. It is also interesting to note that the oxidation of Cu80-Cem20 pellets appears to be characterized by fast kinetics throughout the reaction, with the reaction seemingly complete within 75 s. Conversely, at around the same time mark, the oxidation of Cu50-Ca40-Cem10 appears to be transitioning from a fast reaction phase, to a slower reaction stage, implying that the reaction becomes diffusion-limited at this point. Given that Cu80-Cem20 pellets do not have to contend with the formation of a $CaCO_3$ layer within their structure which would provide a supplementary barrier for O_2 molecules to diffuse through, this is not a surprising observation. Those results lend credence to the theory that the decline of oxidation conversion of composite Cu50-Ca40-

Cem10 pellets was caused by carbonation prior to oxidation. In conclusion, it appears that in the given configuration for biomass gasification (Sequence 2), enhanced carbonation could come at the expense of O_2-carrying capacity. This may have significant implications for the application of this technology for gasification purposes; if the composite pellets cannot maintain a high O_2 uptake, uncoupling the pellets and adopting Sequence 3 might be the best strategy to adopt for this particular scenario.

3.3 Performance of uncoupled pellets in CaL & CLC loops with Sequence 3

By utilizing Sequence 3 where uncoupled pellets are used, the performance of the CuO-based pellets and limestone-based pellets was evaluated with respect to their copper content and calcination conditions respectively.

3.3.1 Effect of Cu content on oxidation conversion and agglomeration of copper-calcium aluminate cement pellets

Copper oxide has been examined as a CLC material by several authors using a variety of supports with different compositions and using several manufacturing techniques including co-precipitation, wet-mixing and impregnation (de Diego et al., 2004). The performance of this material was shown to depend on the Cu content as well as the support and the manufacturing technique. In order to take advantage of the high exothermicity of the oxidation of Cu, it is preferable for the air reactor to be operated at as high a temperature as possible. Although oxidation and calcination were carried out at the relatively mild temperatures of 650°C and 800°C, respectively, up to now, the uncoupling of pellets allows the oxidation of Cu to be carried out at far higher temperatures (950°C or above). This flexibility is owed to the absence of $CaCO_3$

in the air reactor that might otherwise have been calcined. Operating the calciner at higher temperature (920°C) is also desirable because part of the heat is carried by the regenerated limestone pellets back to the gasifier where it contributes in driving the endothermic gasifying process. As well, oxidizing Cu at a higher temperature than the calciner enables the solids to carry some of the heat to the calciner, hereby reducing the amount of fuel required in the latter. However, such temperatures are quite close to the melting point of Cu (1085 °C), and higher than the temperature (900°C) at which maximum thermal softening takes place (Merchant, 2004), making agglomeration a likely scenario. This would be problematic for large scale processes using fluidized bed reactors as agglomeration causes defluidization (Cho et al., 2006). The higher the amount of Cu that can be accommodated in a pellet without agglomeration or loss of oxidation conversion, the lower the total quantity of solids that need to be circulated between the air reactor and calciner.

Homogeneous copper oxide pellets supported with Al_2O_3-based cement were prepared with various CuO contents and evaluated for their oxidation conversion and tendency to agglomerate at the high temperatures. The test conditions and composition of the three batches of pellets are summarized in Table 3.4. Unpelletized, unsupported copper oxide powder was also tested as a "worst-case scenario" for comparison purposes. The TGA profile for a typical oxidation-reduction cycle is shown in Figure 3.10. Examination of this figure reveals a significant mass loss during the inert stage, between the oxidation and reduction stages. This phenomenon was observed for all cycles carried out and occurred because during cooling from 950°C to 920°C in the absence of oxygen, CuO decomposes to Cu_2O as shown in reaction (1.16).

A typical cycle will see about half of the oxygen initially carried by CuO slowly released during its reduction to Cu_2O in the presence of nitrogen, with the other half lost significantly faster during the reduction of the formed Cu_2O to Cu in CO and H_2.

Table 3.4 Summary of experimental conditions for CLC cycles with uncoupled Cu/Al_2O_3-cement based pellets of various Cu content.

	Oxidation	**Reduction**
Temperature (°C)	950	920
Gaseous composition (%)	Air	20% CO, 10% H_2, bal. N_2
Duration (min)	10	10
Particle Size range (μm)	250-600	
Solids Composition	Unsupported copper oxide (Cu100)* Cu80-Cem20 Cu65-Cem35 Cu50-Cem50	

*The unsupported copper oxide used was not in pelletized form, but actually consisted of fine CuO powder, with 98% of particles < 5μm, produced by Aldrich.

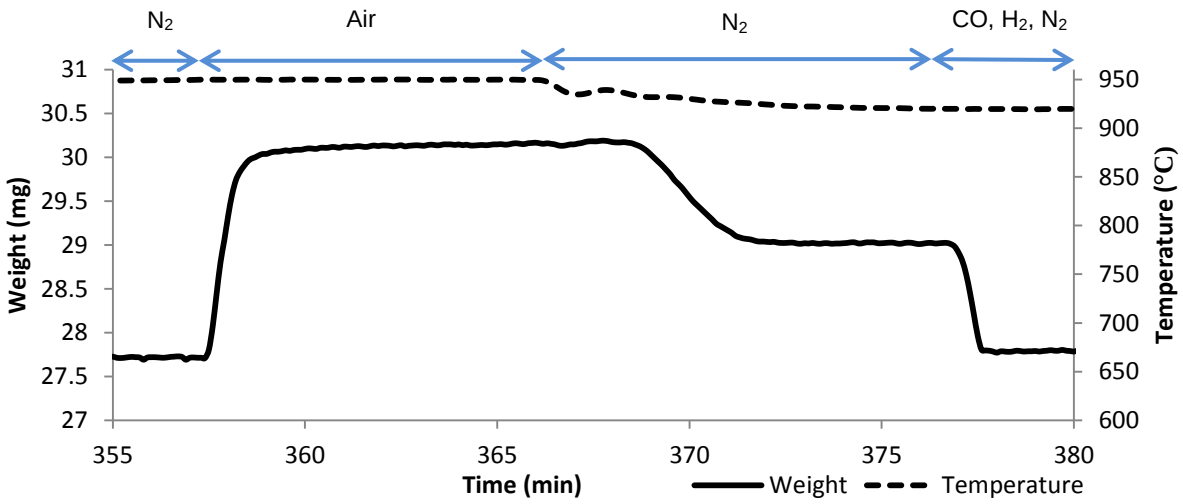

Figure 3.10 The 10th cycle of oxidation and reduction of Cu50-Cem50 pellets

The TGA profile for the oxidation and reduction of Cu65-Cem35 pellets over all 15 cycles is illustrated in Figure 3.11, while the oxidation conversions of all the tested materials over 15 cycles are shown in Figure 3.12. It appears that a higher Cu content is accompanied by a higher propensity to experience a loss in reactivity, as demonstrated by the oxidation conversions of unsupported copper and Cu80-Cem20 pellets. Unsupported copper oxide (Cu100) experienced a dramatic decrease in oxidation conversion within the first 4 cycles, which is consistent with previous results presented in literature (de Diego et al., 2004). Not too surprisingly, pelletizing the Cu using calcium aluminate cement as a support resulted in a far less drastic dip in performance. Cu80-Cem20 pellets exhibited significantly higher oxidation conversion than unsupported CuO powder over all tested cycles, although the conversion was found to gradually decrease with each cycle, reaching 83 % by the 15th cycle. While the Cu80-Cem20 underwent a less radical decrease in oxidation conversion than unsupported Cu, it experienced a loss in reactivity nonetheless. Decreasing the copper content further appeared to eliminate this issue,

with oxidation conversions close to unity achieved. Cu65-Cem35 pellets maintained close to 100% oxidation conversion throughout all 15 cycles. Similarly to Cu65-Cem35 pellets, Cu50-Cem50 pellets exhibited excellent sustained oxidation conversion. The reaction between CuO and Al_2O_3 is known to be quite favorable at temperatures of at least 850°C (de Diego et al. 2005), leading to the formation of copper (II) aluminate ($CuAlO_2$) and copper (I) aluminate ($CuAl_2O_4$) which causes partial loss of CuO (Arjmand et al., 2012). However, calcium aluminate phases have been reported to be easily reducible (Arjmand et al., 2011; Chuang et al., 2008; Gayán, 2011), which might explain why despite the high likelihood of their formation, in this study the pellets still exhibited excellent conversions.

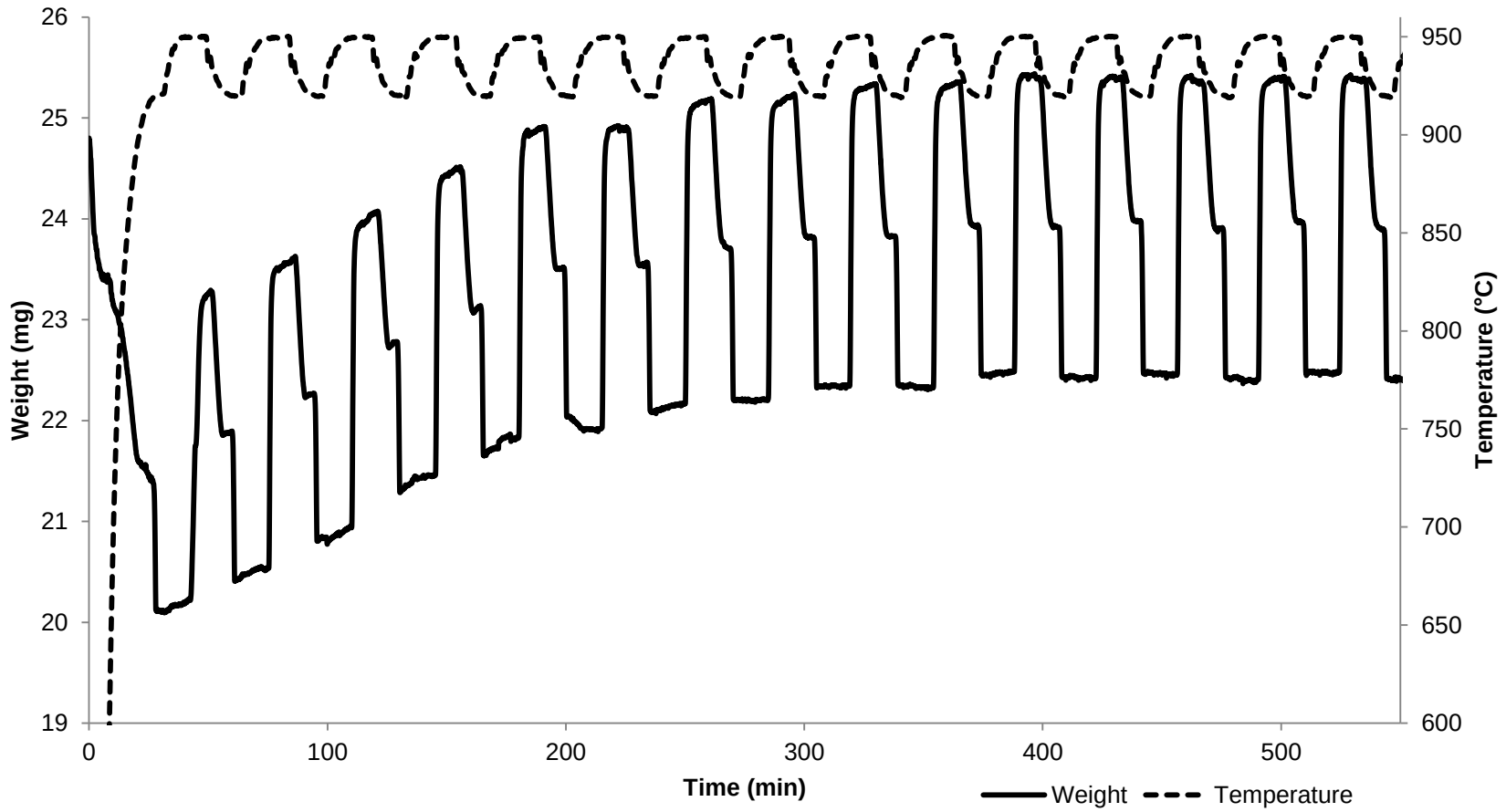

Figure 3.11 TGA profile for oxidation and reduction of Cu65-Cem35 pellets

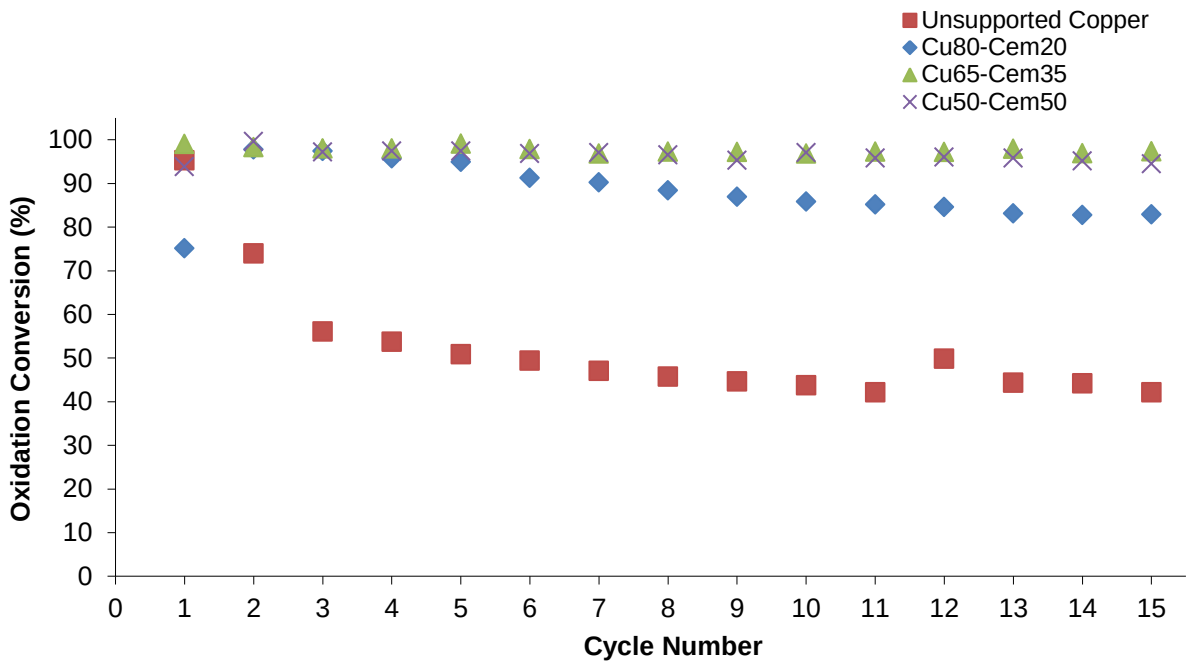

Figure 3.12 Oxidation conversion of unsupported copper, Cu80-Cem20, Cu65-Cem35 and Cu50-Cem50 pellets over 15 cycles

The multi-cycle conversions offer a valuable overview of the sorbent performance over multiple cycles. However, they do not provide any mechanistically-derived explanation for the ability of the different tested pellets to sustain high oxidation conversion. In order to better attempt to explain the differences in various sorbent performance behavior, a comparison of the oxidation conversion with time of all tested materials over the 10th cycle is shown in Figure 3.13.

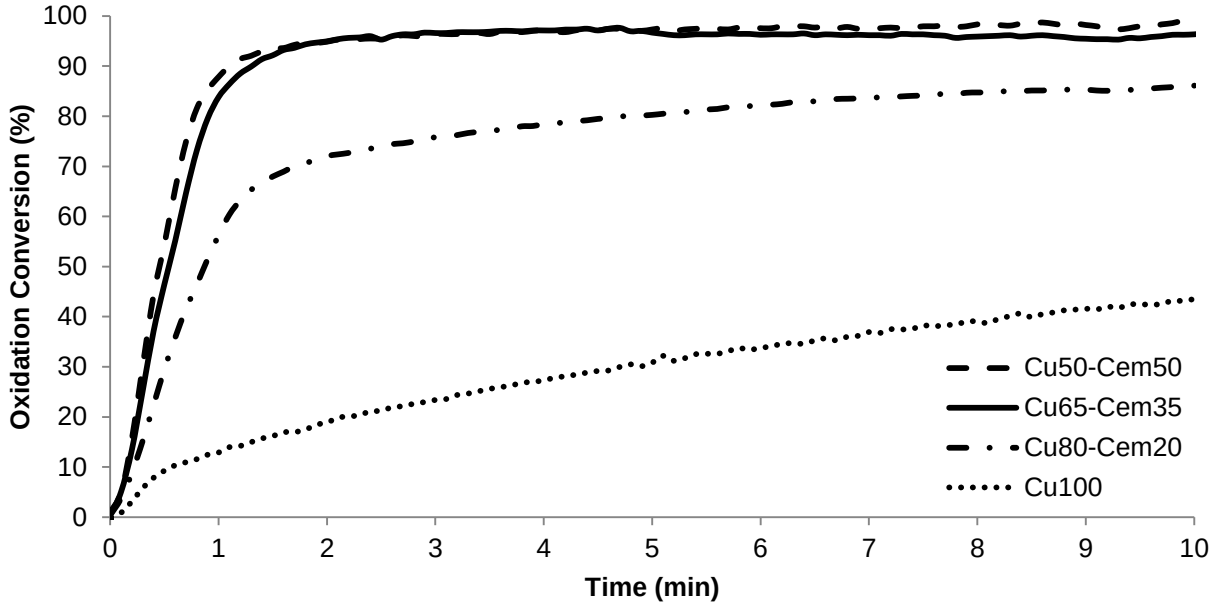

Figure 3.13 Oxidation conversion of 10th cycle for pellets with various Cu content

The pellets with the lowest copper content, Cu50-Cem50 and Cu65-Cem35, exhibited very similar conversion profiles, with oxidation kinetics characterized by a fast reaction stage which accounts for most of the conversion, and a very brief diffusion-controlled stage towards the end of the cycle which lasts for approximately 45 s. The reaction appears to be complete within 2 min. Conversely, the oxidation of Cu80-Cem20 pellets proceeds significantly more slowly than its lower Cu-content counterparts. The reaction and diffusion controlled regimes in the case of Cu80-Cem20 pellets are much more distinguishable, and while the transition from one regime to the other appears to be occurring at the same time mark as for Cu50-Cem50 and Cu65-Cem35 pellets, the slower, diffusion-controlled stage proceeds for considerably longer period, such that, by the end of the duration of the oxidation stage, not all of the available Cu has reacted to form CuO. By the 10^{th} cycle, unsupported copper particles exhibited a very brief reaction-controlled

phase (less than 40 seconds) which is followed by a lengthy diffusion-controlled stage. From the conversion profiles obtained, it appears that the relative amounts of copper and binder affect the kinetics of copper oxidation. This is not an altogether too surprising observation. CA-14 used as the binder is rich in alumina and when used in conjunction with limestone results in higher-porosity pellets due to the formation of mayenite (Manovic & Anthony, 2009b). Pelletization of CuO with CA-14 may present analogous benefits. Unsupported CuO (Cu100) and Cu50-Cem50, representing the upper and lower bounds of copper-content respectively, were subjected to BET and BJH analyses to investigate how pelletization with calcium aluminate cement affects the surface area and pore volume of the oxygen carrier. The results are summarized in
Table 3.5.

Table 3.5 Surface area and pore volume of fresh unsupported copper oxide and Cu50-Cem50 pellets

BET Surface Area (m^2/g)		BJH Pore Volume (cm^3/g)	
Cu100	**Cu50-Cem50**	**Cu100**	**Cu50-Cem50**
1.94	3.37	0.0023	0.0083

Both the surface area and BJH pore volume were significantly increased by pelletizing CuO with 50 % of CA-14 cement. It is quite conceivable that the already low surface area of Cu100 particles is further decreased with each further cycle as the particles become more and more sintered, leading to the observed decreasing oxidation conversion. Such an explanation would be congruent with the physical observations of the samples tested at the end of the TGA runs.

As in the case of cyclic oxidation conversion, an increase in calcium aluminate cement also appeared to affect the tendency of copper-based materials to agglomerate when they were exposed to high temperature CLC cycles. Figure 3.14 shows the unsupported copper and the Cu-Cem pellets after 15 CLC cycles.

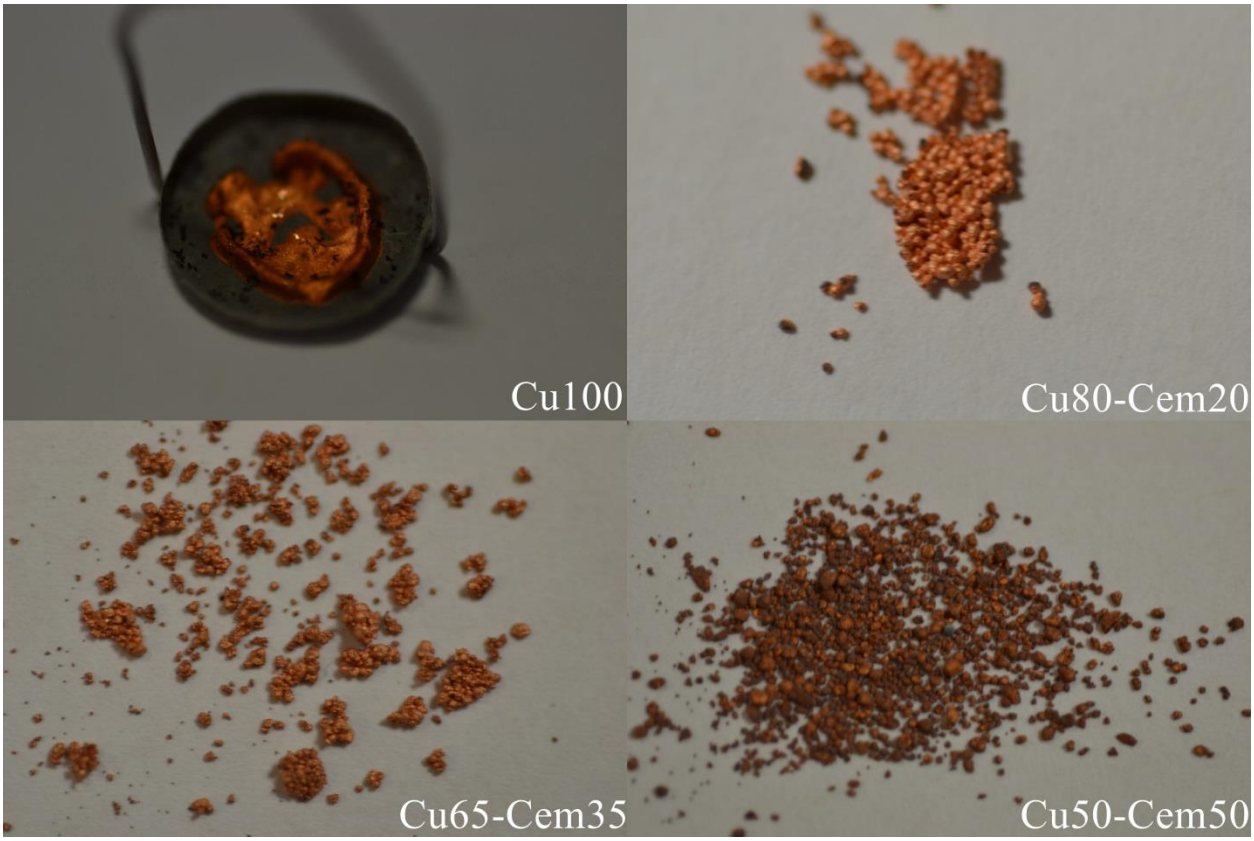

Figure 3.14 Cu-Al_2O_3-based pellets and unsupported copper after 15 CLC cycles

Upon retrieval of the sample from the reactor column, Cu100 particles were found to have fused together, forming a thin disk sticking to the sample pan. While Cu80-Cem20 pellets did not fuse into an undistinguishable mass of copper, as in the case of Cu100, the particles still severely agglomerated and were retrieved from the pan in the form of a disc. Cu65-Cem35 pellets were found to have formed particle clusters, although the exhibited agglomeration was less significant

than in the case of Cu80-Cem20 pellets. Cu50-Cem50 pellets in contrast remained largely unagglomerated.

3.3.2 Effect of Calcination Conditions on Carbonation Conversion of Ca90-Cem10 Pellets

The idea of pelletizing materials was first implemented by combining limestone and calcium aluminate cement solely. Manovic & Anthony (2009a) manufactured several batches of pellets with various compositions and found that the formation of mayenite dispersed across the pellet particles contributed in forming a framework of nanopores which delayed the sintering of CaO sites. The authors concluded that a cement content of 10% was sufficient to considerably improve the reactivity of CaO, but also to significantly enhance the integrity of the material. Contrary to the CuO-based pellets, optimization of the limestone/cement content is therefore not as important for this study as it has been established. What is of particular interest, however, is the influence of the regeneration conditions on the carbonation conversion of the limestone pellets as well as their performance upon carbonation in the presence of syngas.

The regeneration of CaO through CLC, irrespective of the sequence used, will subject the sorbent to a different calcining environment than the one encountered by means of regeneration through oxyfuel combustion. Syngas releases a considerable amount of steam upon reacting with CuO, which could allow operating the calciner at a lower temperature. Of even greater consequence though, is the fact there is a net production of steam from the gasifier. In the context of an integrated process where the produced gas from the gasifier would be used as fuel

in the regenerator, it would be inefficient to condense the steam formed, as it would result in a lower temperature stream sent to the high-temperature calciner. The lack of a condensing unit at the exit of the gasifier implies that significant amount of steam will be fed to the calciner in addition to the steam formed through copper oxide reduction.

The effect of the individual presences of CO_2 and H_2O during calcination on the reactivity of CaO has been investigated by several researchers. Bhatia & Perlmutter (1983) calcined limestone in 100 % N_2, 10 % CO_2 in N_2, and 20 % CO_2 in N_2 at a temperature of 910°C to investigate the effect of CO_2 during calcination on the generated pore structure of the sorbent. They showed than an increase in CO_2 concentration yielded a greater mean pore size and a smaller pore size distribution. In the same study, they reported that calcination with 20% CO_2 resulted in CaO having a more crystalline structure than when the sorbent is calcined in N_2 solely, which could explain why the sorbent is more reactive in the latter case. Borgwardt (1989) reported that calcination in the presence of CO_2 resulted in a loss of porosity and surface area, and a corresponding increase in the rate of CaO sintering. While the presence of CO_2 is almost unanimously deemed to enhance sintering of the sorbent and hence cause a loss in reactivity, a clear consensus has not been reached in the case of steam. Borgwardt (1989) reported that, similarly to CO_2, the presence of steam had a deleterious effect on CaO reactivity, while the combined presence of H_2O and CO_2 affected the reactivity of CaO to an even greater extent than when each gaseous species was present individually in the calcining atmosphere. A few recent works contradict these findings. Wang et al. (2008) calcined limestone (250-500 μm) with increasing amounts of steam in CO_2 and reported a higher CaO reactivity compared to CaO

regenerated in the absence of steam. Donat et al. (2012) observed that a steam concentration as low as 1 % increased the carbonation reactivity of four naturally-occurring limestones, but did not notice any further improvement in performance at higher steam concentrations. Champagne et al. (2013) investigated the performance of Cadomin limestone (250-425 μm) when calcined in 60 % CO_2 and various concentrations of steam (balance N_2) and reported an optimum H_2O content of 15 % where the sorbent exhibited the highest reactivity.

In this work, the Ca90-Cem10 pellets behavior was investigated in a gaseous and thermal environment approaching that encountered in a real calciner/regenerator (which involves the presence of CO_2, H_2O, H_2 and CO). The results were then compared to the carbonation conversion to when the pellets are calcined in conditions typical of oxyfuel combustion. The experimental conditions tested are summarized in Table 3.6.

Table 3.6 Experimental conditions for CaL cycles using Ca90-Cem10 pellets with various calcination conditions

	Carbonation	**Calcination**
Temperature (°C)	650	920
Gaseous composition (Vol. %)	8% CO_2, 22% CO, 11% H_2, 44% H_2O, bal. N_2	100 % N_2
		20% CO, 10% H_2, bal. N_2
		20% CO, 10% H_2, 30 % CO_2, 30 % H_2O, bal. N_2
		90% CO_2, bal. N_2
Duration (min)	15	5
Particle Size Range (μm)	250-600	
Pellet Composition	Ca90-Cem10	

For all four runs carried out, the carbonating mixture consisted of CO_2, CO, H_2 and H_2O, simulating gasifying conditions. Carbonation was carried out at the typical temperature of 650°C. Calcination was carried out at 920°C for all the tested runs, the same temperature employed in the CLC cycles for Sequence 3. Four different calcinations atmospheres were tested. One run involved calcination performed in the presence of CO_2, H_2O, CO, and H_2, simulating the most realistic scenario in the calciner. A mixture of 90% CO_2 and balance N_2 was used to simulate oxyfuel combustion. Given that calcination/reduction was performed only in the presence of CO and H_2 for Cu50-Ca40-Cem10 in Sequence 2 and for CuO-based pellets on the CLC side for Sequence 3, Ca90-Cem10 pellets were also tested at this baseline condition. Furthermore, calcination in N_2 was carried out to simulate milder testing conditions, but also to provide a comparison basis to evaluate any effect of CO and H_2 on the pellets performance. The carbonation conversion over all 15 tested cycles for all four runs is shown on Figure 3.15.

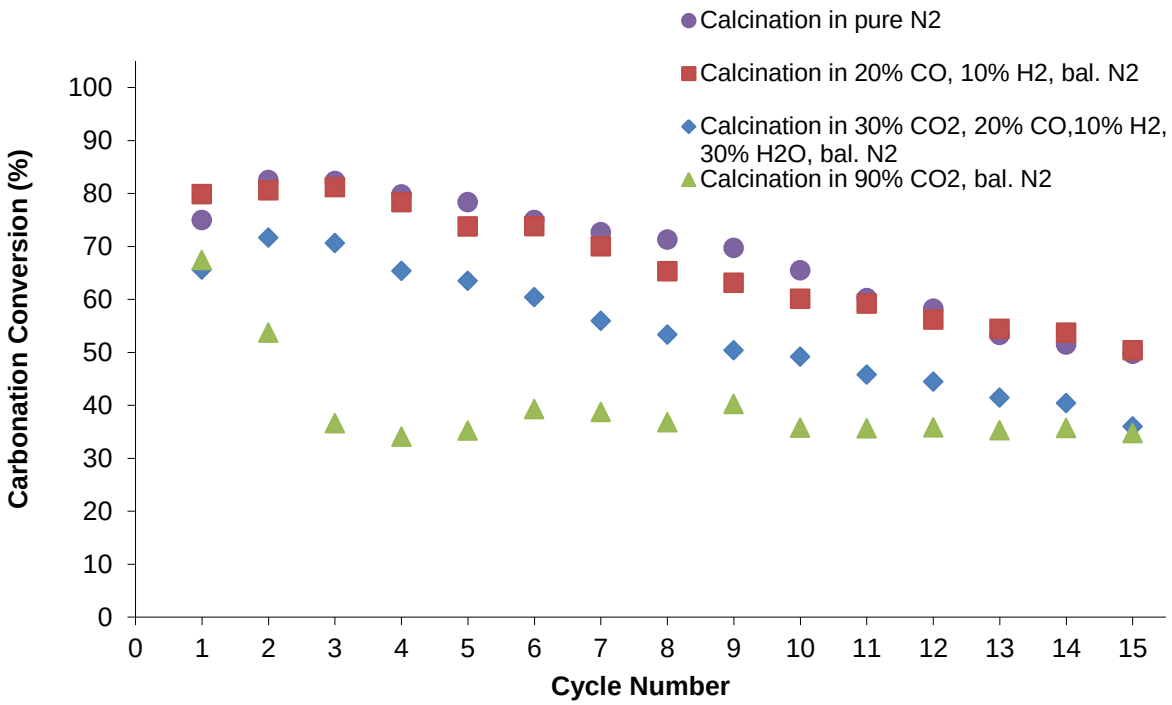

Figure 3.15 Carbonation conversion of Ca90-Cem10 pellets at various calcination conditions

Upon comparison with calcination in pure N_2, the presence of CO and H_2 during calcination did not appear to have any significant incidence on the carbonation conversion over 15 cycles. Under those two calcination conditions, the pellets experienced a gradual decrease in carbonation conversion which still amounted to higher than 50% by the 15th cycle, a high value considering the high calcination temperature. Since calcination is carried out at the high temperature of 920°C, the Boudouard reaction is unlikely to take place given its exothermic nature, limiting any decomposition of the fed CO to CO_2 which could enhance the sintering effect on the sorbent.

The inclusion of CO_2 and H_2O together with CO and H_2 in the calcining mixture caused a significant decrease in the overall conversion of CaO; although the decay in reactivity follows a similar trend as in the two aforementioned tested calcination conditions, the carbonation conversion at the 15th cycle is 34.7 %, more than 15 % points lower. Any consolidating effect that steam might impose upon the morphology of the sorbent during calcination appears to be more than counterbalanced by the greater presence of CO_2.

Of all the calcination conditions tested, the one simulating oxyfuel combustion yielded the worst performance. Although the final conversion in this case was 34 %, very similar to the one obtained when the calcination mixture was composed of all of CO_2, H_2O, CO and H_2, but the decay was much more pronounced within the first three cycles than for any of the other tested conditions; initially conversion drops sharply from 67.4% for the 1st cycle to 36.6 % by the 3rd cycle. Those results are consistent with the literature and would appear to confirm the tendency of CO_2 to enhance sintering of CaO. However, the general trend in the decline of CaO reactivity for the oxyfuel combustion case differs from the other tested cases; after the 4th cycle, a very stable carbonation conversion is maintained throughout the remainder of the cycles. This contrasts with all the other tested cases where, by the 15th cycle, the pellets are still experiencing a steady decline in carbonation conversion.

It is interesting to note that despite the high temperature of 920°C used, Ca90-Cem10 pellets exhibited slightly higher carbonation conversions than composite Cu50-Ca40-Cem10 pellets calcined at the mild temperature of 800°C for a similar calcination atmosphere. However, while a

calcination temperature of 920°C is expected to lead to a significantly greater extent of sintering than 800°C, a BET analysis suggests important differences in the initial morphology of the two sets of pellets that might account for this observation. The absence of CuO within Ca90-Cem10 pellets results in a very porous structure, as confirmed by characterization through BET which puts the surface area of Ca90-Cem10 pellets at 18.02 m^2/g and BJH pore volume at 0.07 cm^3/g. Although it can be assumed that the porosity of Ca90-Cem10 pellets decreases with each cycle through sintering, they are initially far more porous than Cu50-Ca40-Cem10 pellets which were found to have a surface area of 2.97 m^2/g and BJH pore volume of 0.035 cm^3/g. The higher surface area of Ca90-Cem10 pellets suggests that they have a larger number of CaO sites available for carbonation compared to Cu50-Ca40-Cem10 pellets.

Chapter 4 Conclusions and Recommendation

The aim of this work was to investigate the feasibility of different sequences for solid circulation in order to integrate CaL and CLC for steam gasification of biomass and evaluate the performance of composite CuO/CaO/cement pellets in the chosen configuration, as well as those of CuO-based pellets and limestone-based pellets in the CLC and CaL loops respectively.

Using a TGA, Ca50-Cu40-Cem10 pellets consisting of a CuO-enriched core and a limestone-based shell were carbonated in the presence of CO and H_2 resulting in complete reduction of the CuO within 4 minutes, despite parallel carbonation of the CaO shell. The outcome of this test resulted in the elimination of Sequence 1 (oxidation, followed by carbonation) as a possible reactor configuration for the integration of CaL and CLC for gasification purposes.

The performance of composite Cu50-Ca40-Cem10 pellets was tested over multiple cycles at various carbonation compositions. In order to use composite CaO-CuO-Al_2O_3-based cement pellets in an integrated CaL-CLC process for biomass gasification, the solids must be circulated according to Sequence 2, which entails the oxidation of Cu within the pellets to be preceded by the carbonation stage. Homogeneous Ca50-Cu40-Cem10 pellets were tested in this configuration in various carbonation gaseous environments. While the pellets exhibited reasonably high carbonation conversion, albeit with the typical decrease characteristic of limestone-based sorbents, the oxidation conversion also underwent a decrease with the number of cycles, a surprising observation. It appears that carbonation of the pellets prior to oxidation leads to a gradual decrease in the oxidation conversion, especially in the presence of steam, CO and H_2,

plausibly due to the formation of a voluminous layer of $CaCO_3$ blocking the pathway of O_2 molecules on their way to Cu grains. Uncoupling the CaO and Cu species into separate CaO and Cu-based pellets and circulating the solids according to Sequence 3 was thus found to represent a solution to this problem.

Cu-Al_2O_3-based cement pellets with different Cu contents were tested in CLC cycles at high temperature, with Cu50-Cem50 showing excellent oxidation conversion and minimal agglomeration. Experiments were also performed on the CaL side of Sequence 3 using Ca90-Cem10 pellets at various calcination gaseous compositions at high temperature. Ca90-Cem10 pellets were far more porous than composite Cu-Ca-cement pellets. The lowest residual carbonation conversion after 15 cycles was 34 %, corresponding to calcination condition simulating oxyfuel combustion conditions. Calcination in CO_2, H_2O, CO and H_2 (gases all likely to be present in a real-life process involving the dual-loop process) resulted in a decay that was far slower than for the oxyfuel combustion case. However, this slower decline in carbonation conversion was still ongoing by the 15^{th} cycle, whereas the carbonation conversion in the oxyfuel combustion case appeared to have reached a lower bound by the 4^{th} cycle. The presence of CO and H_2 did not have any apparent adverse effect on the reactivity of CaO.

The following is a list of recommendations for future work involving the integration of chemical looping combustion and calcium looping:

- In order to quantify and compare the changes in porosity and surface area of both Cu50-Ca40-Cem10 and Ca90-Cem10 pellets over several cycles, tube furnace experiments

should be carried out so that sufficient material can be gathered for BET N_2 physisorption.

- Given the questionable performance of composite Cu/CaO/Cement pellets using Sequence 2, future efforts at integrating CaL and CLC should be focused on Sequence 3, if only for purposes of biomass gasification. While the conducted work helped in determining the individual performances of limestone-pellets and CuO- based pellets by testing them separately from each other, it would be of particular interest to test the two types of pellets together in a fixed bed and investigate any interaction of the two active components during the high temperature calcination/reduction, which is the only stage at which the limestone-pellets and CuO-based pellets are in contact. Any tendency for the limestone-based pellets to agglomerate with the Cu-based pellet will prove problematic, as it will make subsequent separation of the components even more challenging.

- Cu50-Cem50 pellets exhibited both high cyclic reactivity and a low tendency to agglomerate. A cement content of 50%, however, implies that a significant amount of inert material needs to be circulated across the air reactor and calciner, and constitutes extra material to heat. In order to further optimize the pellets and increase its oxygen-carrying capacity, part of the support could be substituted for another oxygen carrier such as Fe_2O_3. Although the oxygen-carrying capacity of Fe_2O_3 is much lower than that of CuO, Fe_2O_3 is a highly abundant, and hence cheap material, has a high melting point (1594 °C) and, similarly to CuO, exhibits an exothermic reduction with all of CO, H_2 and

CH_4 (Adanez et al., 2011). A significant amount of binder still needs to be present in the pellet, and a good starting point would involve 50% CuO, 25% Fe_2O_3 and 25 % cement.

- Attrition tests should be carried out on the pellets used in this work to gauge their attrition resistance. Given the relatively high cost and toxicity of CuO compared to the other materials used in this work, attrition in the case of CuO-based pellets in particular needs to be minimized.

- Although unaccounted for in this work, the effects of impurities such as sulfur and chlorine, which will be evolved as H_2S and HCl in the gasifier, should be evaluated. Since the proposed process would use the produced gas from the gasifier to fuel the reduction of CuO in the regenerator, those impurities could also be present in the latter. Therefore, the effects of the impurities on CaO and CuO reactivities in the carbonator and calciner respectively could both be investigated.

References

Abanades, J. Carlos, Edward J. Anthony, Dennis Y. Lu, Carlos Salvador, and Diego Alvarez. 2004. "Capture of CO2 from Combustion Gases in a Fluidized Bed of CaO." *AIChE Journal* 50 (7): 1614–22.

Abanades, J. Carlos, G. Grasa, M. Alonso, N. Rodriguez, Edward J. Anthony, and Luis M. Romeo. 2007. "Cost Structure of a Postcombustion CO2 Capture System Using CaO." *Environmental Science & Technology* 41 (15): 5523–27.

Adanez, Juan, Alberto Abad, Francisco Garcia-Labiano, Pilar Gayan, and Luis F. de Diego. 2011. "Progress in Chemical-Looping Combustion and Reforming Technologies." *Progress in Energy and Combustion Science*.

Antal, Michael J., W.E. Edwards, H.L. Friedman, and R.E. Rogers. 1984. *A Study of the Steam Gasification of Organic Wastes.* Cincinnati, OH :: U.S. Environmental Protection Agency, Industrial Environmental Research Laboratory :

Arias, B., G. Grasa, J. C. Abanades, V. Manovic, and E. J. Anthony. 2012. "The Effect of Steam on the Fast Carbonation Reaction Rates of CaO." *Industrial & Engineering Chemistry Research* 51 (5): 2478–82.

Arjmand, Mehdi, Abdul-Majeed Azad, Henrik Leion, Anders Lyngfelt, and Tobias Mattisson. 2011. "Prospects of Al2O3 and MgAl2O4 -Supported CuO Oxygen Carriers in Chemical-Looping Combustion (CLC) and Chemical-Looping with Oxygen Uncoupling (CLOU)." *Energy & Fuels* 25 (11): 5493–5502.

Arjmand, Mehdi, Abdul-Majeed Azad, Henrik Leion, Tobias Mattisson, and Anders Lyngfelt. 2012. "Evaluation of CuAl2O4 as an Oxygen Carrier in Chemical-Looping Combustion." *Industrial & Engineering Chemistry Research* 51 (43): 13924–34.

Baker, E. H. 1962. "87. The Calcium Oxide–carbon Dioxide System in the Pressure Range 1—300 Atmospheres." *Journal of the Chemical Society (Resumed)*, 464–70.

Bhatia, S. K., and D. D. Perlmutter. 1983. "Effect of the Product Layer on the Kinetics of the CO2-Lime Reaction." *AIChE Journal* 29 (1): 79–86.

Blamey, J., E.J. Anthony, J. Wang, and P.S. Fennell. 2010. "The Calcium Looping Cycle for Large-Scale CO2 Capture." *Progress in Energy and Combustion Science* 36 (2): 260–79.

Boot-Handford, Matthew E., Juan C. Abanades, Edward J. Anthony, Martin J. Blunt, Stefano Brandani, Niall Mac Dowell, José R. Fernández, et al. 2013. "Carbon Capture and Storage Update." *Energy & Environmental Science* 7 (1): 130–89.

Borgwardt, Robert H. 1989. "Calcium Oxide Sintering in Atmospheres Containing Water and Carbon Dioxide." *Industrial & Engineering Chemistry Research* 28 (4): 493–500.

Buhre, B.J.P., L.K. Elliott, C.D. Sheng, R.P. Gupta, and T.F. Wall. 2005. "Oxy-Fuel Combustion Technology for Coal-Fired Power Generation." *Progress in Energy and Combustion Science* 31 (4): 283–307.

Canadell, J.G., C. Le Quéré, M.R. Raupach, C.B. Field, E.T. Buitenhuis, P. Ciais, T.J. Conway, N.P. Gillett, R.A. Houghton, and G. Marland. 2007. "Contributions to Accelerating Atmospheric CO2 Growth from Economic Activity, Carbon Intensity, and Efficiency of Natural Sinks." *Proceedings of the National Academy of Sciences of the United States of America* 104 (47): 18866–70.

Champagne, Scott, Dennis Y. Lu, Arturo Macchi, Robert T. Symonds, and Edward J. Anthony. 2013. “Influence of Steam Injection during Calcination on the Reactivity of CaO-Based Sorbent for Carbon Capture.” *Industrial & Engineering Chemistry Research* 52 (6): 2241–46.

Cho, Paul, Tobias Mattisson, and Anders Lyngfelt. 2006. “Defluidization Conditions for a Fluidized Bed of Iron Oxide-, Nickel Oxide-, and Manganese Oxide-Containing Oxygen Carriers for Chemical-Looping Combustion.” *Industrial & Engineering Chemistry Research* 45 (3): 968–77.

Chuang, S, J Dennis, A Hayhurst, and S Scott. 2008. “Development and Performance of Cu-Based Oxygen Carriers for Chemical-Looping Combustion.” *Combustion and Flame* 154 (1-2): 109–21.

Ciferno, Jared P., and John J. Marano. 2002. “Benchmarking Biomass Gasification Technologies for Fuels, Chemicals and Hydrogen Production.” *US Department of Energy. National Energy Technology Laboratory*.

Couto, Nuno, Abel Rouboa, Valter Silva, Eliseu Monteiro, and Khalid Bouziane. 2013. “Influence of the Biomass Gasification Processes on the Final Composition of Syngas.” *Energy Procedia*, TerraGreen 13 International Conference 2013 - Advancements in Renewable Energy and Clean Environment, 36: 596–606.

De Diego, Luis F, Francisco García-Labiano, Juan Adánez, Pilar Gayán, Alberto Abad, Beatriz M Corbella, and Jose María Palacios. 2004. “Development of Cu-Based Oxygen Carriers for Chemical-Looping Combustion.” *Fuel* 83 (13): 1749–57.

De Diego, Luis F., Francisco Garcı´a-Labiano, Pilar Gayán, Javier Celaya, José M. Palacios, and Juan Adánez. 2007. “Operation of a 10 kWth Chemical-Looping Combustor during 200 H with a CuO–Al2O3 Oxygen Carrier.” *Fuel* 86 (7–8): 1036–45.

De Diego, Luis F., Pilar Gayán, Francisco García-Labiano, Javier Celaya, Alberto Abad, and Juan Adánez. 2005. “Impregnated CuO/Al2O3 Oxygen Carriers for Chemical-Looping Combustion: Avoiding Fluidized Bed Agglomeration.” *Energy & Fuels* 19 (5): 1850–56.

Donat, Felix, Nicholas H. Florin, Edward J. Anthony, and Paul S. Fennell. 2012. “Influence of High-Temperature Steam on the Reactivity of CaO Sorbent for CO2 Capture.” *Environmental Science & Technology* 46 (2): 1262–69.

Dou, Binlin, Yongchen Song, Yingguang Liu, and Cong Feng. 2010. “High Temperature CO2 Capture Using Calcium Oxide Sorbent in a Fixed-Bed Reactor.” *Journal of Hazardous Materials* 183 (1-3): 759–65.

Ettouney, Hisham M., Habib I. Shaban, and Lotfy J. Nayfeh. 1995. “Theoretical Analysis of High and Low Temperature Shift Converters.” *Chemical Engineering Communications* 134 (1): 1–16.

Ewan, B.C.R., and R.W.K. Allen. 2005. “A Figure of Merit Assessment of the Routes to Hydrogen.” *International Journal of Hydrogen Energy* 30 (8): 809–19.

Florin, Nicholas H., and Andrew T. Harris. 2008. “Enhanced Hydrogen Production from Biomass with in Situ Carbon Dioxide Capture Using Calcium Oxide Sorbents.” *Chemical Engineering Science* 63 (2): 287–316.

Franco, C., F. Pinto, I. Gulyurtlu, and I. Cabrita. 2003. “The Study of Reactions Influencing the Biomass Steam Gasification Process.” *Fuel* 82 (7): 835–42.

Gokhale, Amit A., James A. Dumesic, and Manos Mavrikakis. 2008. “On the Mechanism of Low-Temperature Water Gas Shift Reaction on Copper.” *Journal of the American Chemical Society* 130 (4): 1402–14.

Grabke, H. J., R. Krajak, E. M. Müller-Lorenz, and S. Strauß. 1996. “Metal Dusting of Nickel-Base Alloys.” *Materials and Corrosion* 47 (9): 495–504.

Herguido, Javier, Jose Corella, and Jose Gonzalez-Saiz. 1992. “Steam Gasification of Lignocellulosic Residues in a Fluidized Bed at a Small Pilot Scale. Effect of the Type of Feedstock.” *Industrial & Engineering Chemistry Research* 31 (5): 1274–82.

Hossain, Mohammad M., and Hugo I. de Lasa. 2008. “Chemical-Looping Combustion (CLC) for Inherent Separations—a Review.” *Chemical Engineering Science* 63 (18): 4433–51.

Hughes, R. W., A. Macchi, D. Y. Lu, and E. J. Anthony. 2009. “Changes in Limestone Sorbent Morphology during CaO-CaCO3 Looping at Pilot Scale.” *Chemical Engineering & Technology* 32 (3): 425–34.

IEA. 2013. *CO2 Emissions From Fuel Combustion Highlights*. Paris: International Energy Agency.

Imtiaz, Qasim, Davood Hosseini, and Christoph Rüdiger Müller. 2013. “Review of Oxygen Carriers for Chemical Looping with Oxygen Uncoupling (CLOU): Thermodynamics, Material Development, and Synthesis.” *Energy Technology* 1 (11): 633–47.

Imtiaz, Qasim, Agnieszka Marta Kierzkowska, and Christoph Rüdiger Müller. 2012. “Coprecipitated, Copper-Based, Alumina-Stabilized Materials for Carbon Dioxide Capture by Chemical Looping Combustion.” *ChemSusChem* 5 (8): 1610–18.

IPCC. 2013. *Climate Change 2013: The Physical Science Basis. Contribution of Working Group I to the Fifth Assessment Report of Intergovernmental Panel on Climate Change*. Cambridge, United Kingdom and New York, NY, USA: Cambridge University Press.

Isaacs, Eddy. 2008. “The Canadian Oil Sands in the Context of the Global Energy Demand.” *Horizon* 110: 232–000.

Ishida, Masaru, and Hongguang Jin. 1994. “A Novel Combustor Based on Chemical-Looping Reactions and Its Reaction Kinetics.” *Journal of Chemical Engineering of Japan* 27 (3): 296–301.

Jain, I. P. 2009. “Hydrogen the Fuel for 21st Century.” *International Journal of Hydrogen Energy*, IWBT 2008 IWBT 2008, 34 (17): 7368–78.

Jerndal, E., T. Mattisson, and A. Lyngfelt. 2006. “Thermal Analysis of Chemical-Looping Combustion.” *Chemical Engineering Research and Design* 84 (9): 795–806.

Kierzkowska, Agnieszka M., and Christoph R. Müller. 2012. “Development of Calcium-Based, Copper-Functionalised CO2 Sorbents to Integrate Chemical Looping Combustion into Calcium Looping.” *Energy & Environmental Science* 5 (3): 6061.

Kumar, Ajay, David D. Jones, and Milford A. Hanna. 2009. “Thermochemical Biomass Gasification: A Review of the Current Status of the Technology.” *Energies* 2 (3): 556–81.

Lu, Dennis Y., Robin W. Hughes, and Edward J. Anthony. 2008. “Ca-Based Sorbent Looping Combustion for CO2 Capture in Pilot-Scale Dual Fluidized Beds.” *Fuel Processing Technology*, Dimethyl Ether Special Section, 89 (12): 1386–95.

Lyon, Richard K, and Jerald A Cole. 2000. “Unmixed Combustion: An Alternative to Fire.” *Combustion and Flame* 121 (1–2): 249–61.

Magelli, Francesca, Karl Boucher, Hsiaotao T. Bi, Staffan Melin, and Alessandra Bonoli. 2009. "An Environmental Impact Assessment of Exported Wood Pellets from Canada to Europe." *Biomass and Bioenergy* 33 (3): 434–41.

Manovic, Vasilije, and Edward J. Anthony. 2009a. "CaO-Based Pellets Supported by Calcium Aluminate Cements for High-Temperature CO2 Capture." *Environmental Science & Technology* 43 (18): 7117–22.

Manovic, Vasilije, and Edward J. Anthony. 2009b. "Long-Term Behavior of CaO-Based Pellets Supported by Calcium Aluminate Cements in a Long Series of CO2 Capture Cycles." *Industrial & Engineering Chemistry Research* 48 (19): 8906–12.

Manovic, Vasilije, and Edward J. Anthony. 2010a. "Lime-Based Sorbents for High-Temperature CO2 Capture—A Review of Sorbent Modification Methods." *International Journal of Environmental Research and Public Health* 7 (8): 3129–40.

Manovic, Vasilije, and Edward J. Anthony. 2010b. "Carbonation of CaO-Based Sorbents Enhanced by Steam Addition." *Industrial & Engineering Chemistry Research* 49 (19): 9105–10.

Manovic, Vasilije, and Edward J. Anthony. 2011a. "CaO-Based Pellets with Oxygen Carriers and Catalysts." *Energy & Fuels* 25 (10): 4846–53.

Manovic, Vasilije, and Edward J. Anthony. 2011b. "Integration of Calcium and Chemical Looping Combustion Using Composite CaO/CuO-Based Materials." *Environmental Science & Technology* 45 (24): 10750–56.

Manovic, Vasilije, Edward J. Anthony, and Dennis Y. Lu. 2008. "Sulphation and Carbonation Properties of Hydrated Sorbents from a Fluidized Bed CO2 Looping Cycle Reactor." *Fuel* 87 (13–14): 2923–31.

Manovic, Vasilije, Jean-Pierre Charland, John Blamey, Paul S. Fennell, Dennis Y. Lu, and Edward J. Anthony. 2009. "Influence of Calcination Conditions on Carrying Capacity of CaO-Based Sorbent in CO2 Looping Cycles." *Fuel* 88 (10): 1893–1900.

Manovic, Vasilije, Yinghai Wu, Ian He, and Edward J. Anthony. 2011a. "Core-in-Shell CaO/CuO-Based Composite for CO2 Capture." *Industrial & Engineering Chemistry Research* 50 (22): 12384–91.

Merchant, H. D. 2004. "Thermal Effects in Thin Copper Foil." *Journal of Electronic Materials* 33 (1): 83–88.

Olajire, Abass A. 2010. "CO2 Capture and Separation Technologies for End-of-Pipe Applications – A Review." *Energy* 35 (6): 2610–28.

Pilar Gayán, Carmen R. Forero. 2011. "Effect of Support on the Behavior of Cu-Based Oxygen Carriers during Long-Term CLC Operation at Temperatures above 1073 K." *Energy & Fuels* 25 (3).

Qin, Changlei, Junjun Yin, Wenqiang Liu, Hui An, and Bo Feng. 2012. "Behavior of CaO/CuO Based Composite in a Combined Calcium and Copper Chemical Looping Process." *Industrial & Engineering Chemistry Research*, September, 120911135600000.

Qin, Changlei, Junjun Yin, Cong Luo, Hui An, Wenqiang Liu, and Bo Feng. 2013. "Enhancing the Performance of CaO/CuO Based Composite for CO2 Capture in a Combined Ca–Cu Chemical Looping Process." *Chemical Engineering Journal* 228 (July): 75–86.

Ramachandran, Ram, and Raghu K. Menon. 1998. "An Overview of Industrial Uses of Hydrogen." *International Journal of Hydrogen Energy* 23 (7): 593–98.

Rochelle, G. T. 2009. “Amine Scrubbing for CO2 Capture.” *Science* 325 (5948): 1652–54.

Romeo, Luis M., Irene Bolea, and Jesús M. Escosa. 2008. “Integration of Power Plant and Amine Scrubbing to Reduce CO2 Capture Costs.” *Applied Thermal Engineering* 28 (8–9): 1039–46.

Salinger, M. James. 2005. “Climate Variability and Change: Past, Present and Future–an Overview.” *Climatic Change* 70 (1-2): 9–29.

Sun, P., J. R. Grace, C. J. Lim, and E. J. Anthony. 2007. “The Effect of CaO Sintering on Cyclic CO2 Capture in Energy Systems.” *AIChE Journal* 53 (9): 2432–42.

Symonds, Robert T., Dennis Y. Lu, Arturo Macchi, Robin W. Hughes, and Edward J. Anthony. 2009. “CO2 Capture from Syngas via Cyclic Carbonation/calcination for a Naturally Occurring Limestone: Modelling and Bench-Scale Testing.” *Chemical Engineering Science* 64 (15): 3536–43.

Turn, S., C. Kinoshita, Z. Zhang, D. Ishimura, and J. Zhou. 1998. “An Experimental Investigation of Hydrogen Production from Biomass Gasification.” *International Journal of Hydrogen Energy* 23 (8): 641–48.

Turn, S. Q. 1999. “Biomass Integrated Gasifier Combined Cycle Technology: Application in the Cane Sugar Industry.” *International Sugar Journal (Worldwide Sugar Edition)* 101 (1205;1206;1207): 267–272;316–322;368–374.

Udomsirichakorn, Jakkapong, and P. Abdul Salam. 2014. “Review of Hydrogen-Enriched Gas Production from Steam Gasification of Biomass: The Prospect of CaO-Based Chemical Looping Gasification.” *Renewable and Sustainable Energy Reviews* 30 (February): 565–79.

Walawender, Walter P., Deborah A. Hoveland, and L. T. Fan. 1985. “Steam Gasification of Pure Cellulose. 1. Uniform Temperature Profile.” *Industrial & Engineering Chemistry Process Design and Development* 24 (3): 813–17.

Wang, Yin, Shiying Lin, and Yoshizo Suzuki. 2008. “Limestone Calcination with CO 2 Capture (II): Decomposition in CO 2/Steam and CO 2/N 2 Atmospheres.” *Energy & Fuels* 22 (4): 2326–31.

Xu, Lei, Jianan Wang, Zhenshan Li, and Ningsheng Cai. 2013. “Experimental Study of Cement-Supported CuO Oxygen Carriers in Chemical Looping with Oxygen Uncoupling (CLOU).” *Energy & Fuels* 27 (3): 1522–30.

Yang, Shaojun, and Yunhan Xiao. 2008. “Steam Catalysis in CaO Carbonation under Low Steam Partial Pressure.” *Industrial & Engineering Chemistry Research* 47 (12): 4043–48.